

PLOS Computational Biology

Cannabinoids Disrupt Memory Encoding by Functionally Isolating Hippocampal CA1 from CA3

--Manuscript Draft--

Manuscript Number:	PCOMPPBIOL-D-16-02044R1
Full Title:	Cannabinoids Disrupt Memory Encoding by Functionally Isolating Hippocampal CA1 from CA3
Short Title:	Cannabinoids Disrupt Memory Encoding by Functionally Isolating Hippocampal CA1 from CA3
Article Type:	Research Article
Keywords:	hippocampus, cannabinoids, THC, memory, dnms, CA3, CA1
Corresponding Author:	Roman Sandler UCLA Los Angeles, UNITED STATES
Corresponding Author Secondary Information:	
Corresponding Author's Institution:	UCLA
Corresponding Author's Secondary Institution:	
First Author:	Roman A Sandler
First Author Secondary Information:	
Order of Authors:	Roman A Sandler Dustin Fetterhoff Robert E Hampson Sam A Deadwyler Vasilis Z Marmarelis
Order of Authors Secondary Information:	
Abstract:	Much of the research on cannabinoids (CBs) has focused on their effects at the molecular and synaptic level. However, the effects of CBs on the dynamics of neural circuits remains poorly understood. This study aims to disentangle the effects of CBs on the functional dynamics of the hippocampal Schaffer collateral synapse by using data-driven nonparametric modeling. Multi-unit activity was recorded from rats doing a working memory task in control sessions and under the influence of exogenously administered tetrahydrocannabinol (THC), the primary CB found in marijuana. It was found that THC left firing rate unaltered and only slightly reduced theta oscillations. Multivariate autoregressive models, estimated from spontaneous spiking activity, were then used to describe the dynamical transformation from CA3 to CA1. They revealed that THC served to functionally isolate CA1 from CA3 by reducing feedforward excitation and theta information flow. The functional isolation was compensated by increased feedback excitation within CA1, thus leading to unaltered firing rates. Finally, both of these effects were shown to be correlated with memory impairments in the working memory task. By elucidating the circuit mechanisms of CBs, these results help close the gap in knowledge between the cellular and behavioral effects of CBs.
Suggested Reviewers:	Berj Bardakjian University of Toronto

	<p>berj@cbl.utoronto.ca</p> <p>Jonathan Victor Cornell University jdvicto@med.cornell.edu</p> <p>Gregory Brewer University of California Irvine gjbrewer@uci.edu</p> <p>Thomas Demarse University of Florida tdemarse@bme.ufl.edu</p>
Opposed Reviewers:	
Additional Information:	
Question	Response
Financial Disclosure	<p>This work was supported by National Institute of Health (www.nih.gov) grant P41-EB001978 to the Biomedical Simulations Resource at the University of Southern California.</p> <p>The funders had no role in study design, data collection and analysis, decision to publish, or preparation of the manuscript</p> <p>Please describe all sources of funding that have supported your work. This information is required for submission and will be published with your article, should it be accepted. A complete funding statement should do the following:</p> <p>Include grant numbers and the URLs of any funder's website. Use the full name, not acronyms, of funding institutions, and use initials to identify authors who received the funding.</p> <p>Describe the role of any sponsors or funders in the study design, data collection and analysis, decision to publish, or preparation of the manuscript. If the funders had no role in any of the above, include this sentence at the end of your statement: <i>"The funders had no role in study design, data collection and analysis, decision to publish, or preparation of the manuscript."</i></p> <p>However, if the study was unfunded, please provide a statement that clearly indicates this, for example: <i>"The author(s) received no specific funding for this work."</i></p>
* typeset	
Competing Interests	The authors have declared that no competing interests exist
You are responsible for recognizing and disclosing on behalf of all authors any competing interest that could be perceived to bias their work, acknowledging all financial support and any other relevant financial or non-financial competing interests.	

<p>Do any authors of this manuscript have competing interests (as described in the PLOS Policy on Declaration and Evaluation of Competing Interests)?</p>	
<p>If yes, please provide details about any and all competing interests in the box below. Your response should begin with this statement: <i>I have read the journal's policy and the authors of this manuscript have the following competing interests:</i></p>	
<p>If no authors have any competing interests to declare, please enter this statement in the box: "The authors have declared that no competing interests exist."</p>	
<p>* typeset</p>	
<p>Data Availability</p> <p>PLOS journals require authors to make all data underlying the findings described in their manuscript fully available, without restriction and from the time of publication, with only rare exceptions to address legal and ethical concerns (see the PLOS Data Policy and FAQ for further details). When submitting a manuscript, authors must provide a Data Availability Statement that describes where the data underlying their manuscript can be found.</p> <p>Your answers to the following constitute your statement about data availability and will be included with the article in the event of publication. Please note that simply stating 'data available on request from the author' is not acceptable. If, however, your data are only available upon request from the author(s), you must answer "No" to the first question below, and explain your exceptional situation in the text box provided.</p> <p>Do the authors confirm that all data underlying the findings described in their manuscript are fully available without restriction?</p>	<p>Yes - all data are fully available without restriction</p>
<p>Please describe where your data may be found, writing in full sentences. Your answers should be entered into the box below and will be published in the form you provide them, if your manuscript is</p>	<p>All data will be posted in a public repository on the USC BMSR website (https://bmsr.usc.edu) after publication of article.</p>

accepted. If you are copying our sample text below, please ensure you replace any instances of **XXX** with the appropriate details.

If your data are all contained within the paper and/or Supporting Information files, please state this in your answer below. For example, "All relevant data are within the paper and its Supporting Information files."

If your data are held or will be held in a public repository, include URLs, accession numbers or DOIs. For example, "All **XXX** files are available from the **XXX** database (accession number(s) **XXX**, **XXX**)."
If this information will only be available after acceptance, please indicate this by ticking the box below.

If neither of these applies but you are able to provide details of access elsewhere, with or without limitations, please do so in the box below. For example:

"Data are available from the **XXX** Institutional Data Access / Ethics Committee for researchers who meet the criteria for access to confidential data."

"Data are from the **XXX** study whose authors may be contacted at **XXX**."

* typeset

Additional data availability information:

Tick here if the URLs/accession numbers/DOIs will be available only after acceptance of the manuscript for publication so that we can ensure their inclusion before publication.

Cannabinoids Disrupt Memory Encoding by Functionally Isolating Hippocampal CA1 from CA3

Roman A. Sandler¹, Dustin Fetterho², Robert E. Hampson², Sam A. Deadwyler² & Vasilis Z. Marmarelis¹

¹ Department of Biomedical Engineering, University of Southern California, Los Angeles, CA, USA

² Department of Physiology & Pharmacology, Wake Forest University, Winston-Salem, NC, USA

Research into cannabinoids (CBs) over the last several decades has found that they induce a large variety of oftentimes opposing effects on various neuronal receptors and processes. Due to this plethora of effects, disentangling how CBs influence neuronal circuits has proven challenging. This paper contributes to this by using data driven modeling to examine how THC affects the input-output relationship in the Schaffer collateral synapse in the hippocampus. It was found that THC functionally isolated CA1 from CA3 by reducing feedforward excitation and theta information flow while simultaneously increasing feedback excitation within CA1. By elucidating the circuit mechanisms of CBs, these results help close the gap in knowledge between the cellular and behavioral effects of CBs.

The use of sophisticated computational and system identification techniques to interpret complex biological datasets makes this paper ideally suited for PLOS Computational Biology. Furthermore, a central theme in the paper is that such techniques can offer neuroscientists greater insight than more conventional techniques. We make an effort to directly compare these techniques in the paper.

Reviewer #1: The authors have applied a novel analysis and interpretation to a study of the effects of THC on behavioral and cellular activity in rats. Based on a decrease in the efficacy and theta modulation of CA3 output to CA1, along with a lack of effect on theta modulation and firing rates in CA1 cells, the authors propose that the two subfields become less coupled when under the influence of THC and suggest that this reaction may explain the behavioral deficits seen in the delayed non-match to sample task when performed by rats under the influence of THC. This interpretation has potential and would be a valuable addition to the literature if it is found to be true. However, it is inconsistently explained and supported within this manuscript, and a part of it is based on incorrect assumptions about CA1 anatomical connectivity. There are concerns in terms of science and writing quality that must be addressed for this work to present a compelling case for its analysis and interpretation.

General Comments: This reviewer has raised excellent points relating to the mismatch between our hypothesis and the current literature. These comments were extremely helpful and have inspired us to review the current literature much more carefully. Thus, we have completely rewritten the paragraph dealing with our proposed hypothesis in the discussion. The new paragraph is found on 286-329. Whether this manuscript will ultimately be accepted in PLOS Computational Biology or not, we are very grateful to this reviewer for helping us make our work much stronger.

Scientific Concerns:

1. Results - Manuscript Page 7, lines 186 - 188: "This confirms previous reports which show ... that CA1 is capable to generating endogenous theta rhythms". It is consistent with the report of Goutagny et al 2009 but does not confirm it - CA1 also receives timed input from sources other than CA3 (ECIII and medial septum are two of the most significant), and there is no reason to discount their input here when the authors have not shown any effect of THC on their spike timing or theta modulation.

Response: This is a valid point. Septal inputs to the hippocampus are particularly important for theta rhythms (for example, see Fuhrmann et al., 2015; Neuron). The language has been made more precise to reflect this: "**This is consistent with previous reports which show that CA3 propagates strong theta rhythms to CA1 [39,40] and also that CA1 is capable to generating endogenous theta rhythms [41].**"

2. Discussion - Manuscript Page 10, lines 295-303. The authors first refer to "increased feedback excitation" but the proposed mechanism given below sounds more like "decreased feedback inhibition" and even includes a contributing factor of decreased CA1 pyramidal input to the inhibitory cells, so the proposed mechanisms are not consistently described or represented throughout the discussion. Relatedly, in the results section (Manuscript page 7, lines 211-212), the authors state "Essentially, the more THC increased feedforward inhibition and feedback excitation, the worse the rodent did on the task", which is also confusing as elsewhere the authors seem to indicate that the feedforward inhibition (anatomically, this should be the CCK+ cell activity) is weakened with THC.

Response: This remark is very helpful. Indeed, the system identification method was able to detect a change in feedback excitatory index in CA1, but it is agnostic as to whether that is caused by reduced feedback inhibition or increased feedback excitation. As the reviewer points out, we hypothesize that it is the former. To make this point more clear, we changed the discussion to read: "**It was found that THC increased feedback excitatory index in CA1 and that the magnitude of this effect was correlated with behavioral deficits. We hypothesize that this is due to reduced feedback inhibition from CA1 cholecystokinin (CCK)-containing basket cells. ...**" Furthermore, the sentence which mentioned increased feedback excitation in the results section was completely removed.

3. Discussion - Manuscript page 10, line 300-301 states in regard to CCK+ cells that "their primary input and output is from/to CA1 pyramidal 301 cells [52]." It is true their primary output is to CA1 pyramidal cells, however it is misleading to state that their primary input is from CA1 pyramidal cells. Reference #52 does not make that claim, speaking only to the proportion of CA1 inputs for all interneuron types together, and in fact this reviewer is not aware of any definitive published evidence for monosynaptic connections from CA1 pyramidal cells to CCK+ basket cells, although there are known connections from CA1 pyramidal cells to other CCK+ cells. It would be more correct to state "their primary output is CA1 pyramidal cells and some types of CCK+ cells also receive input from CA1 pyramidal cells" as shown for example in **Lee et al J Neurosci 2010**.

Response: This point is answered together with point 4 below

4. It follows that the statement "(2) reducing their total amount of action potentials due to reduced glutamatergic input from CA1 pyramidal cells" is probably untrue for CCK+ basket cells, which are the majority of CCK+ cells in CA1. Most CCK+ cells have dendrites in the area of Schaffer Collateral innervation of CA1 and are activated by the afferent Schaffer Collateral input (although some have dendrites within the oriens where most CA1 pyramidal cell collaterals would be found), so a reduction in afferent SC input is far more likely to be responsible for reduced drive to CCK+ cells than a reduction in CA1 pyramidal input and in the case of CCK+ basket cells, this is especially true.

Response: We thank the reviewer for bringing these points to our attention. After looking at the literature more closely we agree that the primary input to CA1 CCK basket cells comes from CA3 rather than CA1 pyramidal cells (Lee et al., 2010; Matyas et al., 2004). Matyas et al., 2004 also showed that 20% of CA1 CCK cells' inputs are in the str. oriens

layer and suggested that these inputs are from CA1 pyramidal collaterals¹. In either case, as the reviewer pointed out, our theory is valid whether the decreased excitatory input comes from CA3 or CA1 pyramidal cells. Both have the net effect of reducing CA1 CCK basket cell activity and thus CA1 feedback inhibition. Thus, we have changed the relevant sentence to: “While CCK cells only make up 13.9% of interneurons (Bezaire et al., 2013), they express significantly more CB1 receptors than any other cell in the hippocampus (Katona et al., 2000), and their primary output is to CA1 pyramidal cells. Increased THC concentrations would reduce CCK interneuron output by (1) reducing the amount of GABA they release per action potential (2) reducing their MFR due to reduced glutamatergic input from principal cells in both CA3 and CA1.”

5. Manuscript Page 10, line 299 - “they express significantly more CB1 receptors than any other cell in the hippocampus [53],” but not all CB1 receptors are created equal; those found on pyramidal cells are thought to be **more** efficacious, so it would be helpful to consider this in addition to the receptor abundance. It would also be helpful to discuss the roles of DSI and DSE in the circuit and the effect of THC on those roles. For background on this and the previous point, check out Ruehle et al J Psychopharmacology 2012 and the references it cites.

Response: We are very grateful that the reviewer brought these sources to our attention. We have elaborated on the point that pyramidal cell CB1 receptors are more efficacious in our discussion: “Even though pyramidal cells have much lower densities of CB1 receptors than interneurons (Katona et al., 2000; Oshno-Shosaki et al., 2002), there is evidence that CB induced reduction of excitation is larger than these relative densities suggest. Principal cells outnumber interneurons 20:1 in CA1 (Ahmed and Mehta, 2009) and their CB1 receptors were found to be several fold more efficacious than those of interneurons (Steindel et al., 2009). Further, lower baseline activation levels of CB1 receptors on principal cells than on interneurons suggest they would be disproportionately activated by CB agonists (Ruehle et al., 2012).”

Writing & readability concerns

The writing level of this manuscript **occasionally** falls below what this reviewer would expect and distracts from the scientific message. It is very fixable. This reviewer recommends:

1. Before revising the manuscript, (re)read a short book on writing or scientific writing. Style: Basics of Clarity and Grace by Joseph Williams is short and very helpful
2. Revise the manuscript, checking especially for the following (only a few examples of each problem are listed here):
 - 2a. The nouns and verbs should be appropriately plural or singular
 - 2ai. Example: Actual Page 9, line 15: synapse should be plural (synapses)
 - 2aii. Example: Manuscript Page 2, line 72-73: “... a type of linear nonparametric models ...” → models should be singular (model)
 - 2aiii. Example: “the emergent effects ... is “ → is should be plural (are)
- 2b. Keep in mind whether something is countable when deciding between using ‘amount’ and some form of ‘number’
- 2bi. Example: Manuscript page 10, line 289 - “THC reduces the amount of casually connected CA3-CA1 290 neuronal pairs”; amount → number, frequency, incidence

Response: We are deeply embarrassed by this and have done our best to improve the language, including reading the paper several times over and getting feedback from several native English speaking peers. All the above examples have been corrected according to the reviewer’s suggestions. We thank the reviewer for bringing them to our attention.

- 2c. The word ‘this’ should rarely stand alone in scientific publications - it is vague and confusing. Better to specify what it means each time
- 2ci. Manuscript Page 1, line 35: “This paper contributes to this by using” → first this (“This paper”) is good. Second one (“contributes to this”) is vague, try something like “This paper contributes to disentangling these effects by using...” which may need to be further refined to make it less awkward

Response: Sentence changed to: “This paper contributes to our understanding of the circuit level effects of CBs by using data driven modeling to examine how THC affects the input-output relationship in the Schaffer collateral synapse in the hippocampus.”

- 2cii. Manuscript Page 2, line 76: “This makes them particularly well suited” → “This characteristic makes...” or “This lack of reliance on assumptions makes ...”

Response: Sentence changed to: “This characteristic makes them particularly well suited ...”

- 2d. Remove unnecessary qualifications and rewrite unprofessional ones differently
- 2di. Example: Manuscript Page 2, line 46: “has attracted a lot of somewhat controversial attention” is distracting because of its imprecision and contrast to most writing found in journal publications

¹ Interestingly, Lee et al., 2014 did not find any evidence of direct connections from CA1 pyramidal cells to CA1 CCK basket cells; however, they had a small sample size and never implied they disproved the possibility of such connections.

Response: Sentence rewritten as “In particular, CB agonists have shown promising but mixed results in the treatment of epilepsy, as various types of agonists at various doses have been shown to be both pro- and anticonvulsant”

2e. Parallel sentence construction

2ei. Example: Manuscript Page 2, line 49: the items in this list do not follow a parallel construction, making it confusing to parse: “much work has been done on the chemical structure of various cannabinoids, cannabinoid receptors, along with their cellular interactions and pharmacology” - would be clearer as “.... on the chemical structure of various cannabinoids and cannabinoid receptors, along with their...” or “... on the chemical structure of various cannabinoids, cannabinoid receptors, and their...”

Response: Sentence changed to “Parallel to increasing therapeutic research, much work has been done on the chemical structure of various cannabinoids and cannabinoid receptors, along with their cellular interactions and pharmacology.”

2f. Word choice is not always the most appropriate

2fi. Example: Manuscript Page 10, lines 320 - 321 “the decrease in feedforward excitation overpowers the increase in feedback excitation and results in lower MFR” - it is difficult to visualize a decrease in agency overpowering something, would be more fitting to say “the increase in ... is unable to compensate for the decrease in ... , resulting in lower MFR” effect/affect

2g. Other recommendations from the writing book

3. Address these other issues as well:

3a. Manuscript page 1, lines 31-40: unclear whether this is an alternate abstract? It repeats its last sentence from the actual abstract

Response: This is a required Author Summary. A title has been added to make this more clear.

3b. Ensure transitions are appropriate - they should respect the flow of logic

3c. Spell check

3d. Appropriate use of commas. Sometimes they are extraneous, other times they are sorely needed:

3di. Example: Manuscript page 3, line 93: “While performing the DNMS task single-unit...” is confusing, add a comma to clarify: “While performing the DNMS task, single-unit...”

Response: Comma has been added.

Minor & other concerns

1. Figure 1B - what are the units on the axes? Assuming Hz for individual firing rates?

Response: Yes, that is correct. The Hz units have been added to the labels to clarify this.

2. Figure 2 caption says “Note that 1 CA1 neuron has no significant inputs.” → please specify that the statement refers to the theoretical model using Granger causality (is not intended as a biological anatomy statement based on experimental observation).

Response: Sentence changed to “Note that 1 CA1 neuron has no significant granger-causal inputs.”

3. Figure 2B could be further clarified with a “CA3 input #1” label over the CA3 spike trains, to correspond to inputs in 2C and a “CA1” label over the CA1 spike train.

Response: The figure has been modified to reflect this

4. Manuscript Page 17, line 575 is confusing: “N-1 two input models were constructed”

Response: Sentence has been changed to: “Afterwards, N-1 models were constructed with two inputs: the previously selected input and one of the remaining potential inputs.”

5. Figure 3 CD - can you add a legend for the animal colors, even if the animal names are arbitrary (“animal 1, 5 sessions; animal 2, 3 sessions; animal 3...”). It would enable readers to quickly understand the color coding w/o having to read the legend and also quickly see how many animals & sessions were included.

Response: A legend was added with the Rat 1, Rat 2, etc... The amount of sessions was added since each animal went through a certain amount of control and THC sessions. In the plots under discussion, each dot represents the difference in a value in one of the THC sessions from the mean of that value in the control sessions. Thus, I think it would be confusing to put in the amount of sessions as the reader wont know whether they refer to just the THC sessions (i.e. the # of dots of that color), or all the sessions.

6. Figure text is quite small - for example, the legend text in Figure 2C is almost unreadable

Response: All figure text was made larger.

7. There should be a short summary of the previous work, at least the categorization of functional cell types (FCTs) that currently refers to previous work for any explanation, to enable this manuscript to stand alone.

Response: This is a great point. We decided that in order to improve clarity and avoid confusion, the reference to FCTs from previous work has been removed. Instead, the paper simply refers to these cells as sample-presentation cells and provides a reference to the previous work which talked about FCTs. We believe that since this is such a minor aspect of the paper, it is preferable not to go into excessive detail on this, as it will distract the reader.

8. Figures should stand alone; spell out abbreviations in the captions (ex: Figure captions should spell out DNMS, FCT, gPDM at least once)

Response: All abbreviations in the figures have been spelled out (except for well known ones such as CA1 and THC).

9. Some references in the bibliography have corrupted characters - see reference 55 for example. Also, the journal names are not properly capitalized; if they are proper in the bib file, simply surround the whole journal title with an extra set of curly braces {} to preserve capitalization in the compiled document

Response: Corrupted characters in bibliography have been corrected, including source 55. All Journal titles have been properly capitalized.

Reviewer #2: In this paper the authors take an interesting and novel approach in applying nonparametric modelling to investigate the effect of exogenous CBS on the hippocampal Schaffer collateral synapse. In my opinion certain points (listed below) merit further clarification.

General feedback: Both this reviewer and reviewer #1 raised excellent points relating to the mismatch between our hypothesis and the current literature. In response to this, we have completely rewritten the paragraph dealing with our proposed hypothesis in the discussion. The new paragraphs are found on lines 286-329. We believe this rewritten section is much more clear and addresses the reviewer's concerns.

Comments

1. CB1 receptors are found on both excitatory and inhibitory cells in hippocampus leading to both suppression of inhibition and excitation. However, depression of inhibition is much more prevalent than the depression of excitation and can be induced with lower CB concentrations, supposedly due to the lower sensitivity of CB1 receptors expressed on excitatory rather than inhibitory synaptic terminals. (See Ohno-Shosaku, T. et al, (2002). Journal of Neuroscience and Zachariou et al 2014 Journal of Computational Neuroscience). My main concern is that this fact is not considered in the model and hypothesis formulation and in the overall results interpretation. For example in a relatively low THC dose the CB1 receptor found on excitatory terminal might not be affected. Hence, the conclusion that "THC functionally isolates CA1 from CA3 by reducing feed forward excitation and theta information flow while simultaneously increasing feedback excitation within CA1" might not necessarily hold. Please discuss/address.

Response: The reviewer's point that DSI is more prevalent than DSE is well taken. Our strongest findings pertained to changes in CA1 feedback, which we believe is due to reduced feedback inhibition from CA1 CCK basket cells (i.e. DSI). We also found evidence for reduced feedforward excitation which we believe is due to DSE. Even though DSE is less prevalent than DSI, there is evidence that in-vivo, DSE may play a more prominent role than previously thought. (this point was made by reviewer #1). We have added the following sentences to discuss this issue: "**Even though pyramidal cells have much lower densities of CB1 receptors than interneurons** (Katona et al., 2000; Oshno-Shosaki et al., 2002), there is evidence that CB induced reduction of excitation is larger than these relative densities suggest. Principal cells outnumber interneurons 20:1 in CA1 (Ahmed and Mehta, 2009) and their CB1 receptors were found to be several fold more efficacious than those of interneurons (Steindel et al., 2009). Further, lower baseline activation levels of CB1 receptors on principal cells than on interneurons suggest they would be disproportionately activated by CB agonists (Ruehle et al., 2012)."

2. The model appears to only describe excitatory cells, as it focuses on the Schaffer collateral synapse. However, in the Methods it is noted that no differentiation was made between principal cells and interneurons. How did the authors ensure that the recorded cells whose activity was considered for fitting the model were indeed excitatory?

Response: This decision was made for two reasons. First, the paper used a 'blackbox' granger-causal framework where it was understood that functionally connected cells are not necessarily anatomically connected and that the estimated feedforward/feedback filters are not physiological EPSPs but rather an abstract measure of influence. Thus, the estimated filters include not only direct neuron-to-neuron physiological processes such as dendritic integration, but also indirect processes such as feedforward inhibition whereby the recorded CA3 neuron activates an unseen CA1 interneuron which activates the recorded CA1 principal cell (Pouille and Scanziani, 2001). Given that our goal was to see how CA3 \rightarrow CA1 dynamics change with THC, and given the high levels of connectivity between CA1 pyramidal cells and interneurons, we felt that this distinction would be somewhat artificial. Second, given that we used in-vivo extracellular recordings, there is no fullproof method to separate pyramidal cells and interneurons. Commonly used methods which rely on MFR, waveform shape, and ISI distributions can only give 'putative pyramidal cells'. We attempted to use a similar procedure by removing cells with MFR >5 Hz as 'putative' interneurons. These cells made up only a minority of our recorded cells and did not significantly alter any of our results. Namely, with only 1 exception, all significant P values remained so even after these cells' exclusion (the exception was for CA3 theta power reduction on line 118 whose P value went from .045 to .062).

3. Figures: All figures would benefit from a larger font size, as currently many parts are not easily readable. In Figure 1 some axis labels and units are missing and the figure would benefit from a longer/more descriptive legend. Also I find figure 1E confusing please clarify which part shows control and which TCH (the extra y axis with THC/control is not that informative). Same holds for Figure 3A and B. In Figure 2B the y-axis is missing (and fonts are very small). Also the color-coding blue - green for control - THC should be repeated at least in every figure (and maybe in sub-figures). Also in Figure 4 each panel should be properly described.

We thank the reviewer for all these suggestions that will certainly add to the readability of the paper. The font sizes of all figures were made bigger. Axis labels and units were added in figure 1. A legend was added to Fig 1E and 3A,B. In Fig.

2, the color schema for CA3 and CA1 was changed to make it distinct from Control/THC. In Fig. 2b, the y-axis is shown for the bottom input, and the caption says that the y-axis and scale is the same for all 3 inputs. The y-axis was not added to the top two inputs for aesthetic reasons.

Bibliography:

Ahmed, Omar J., and Mayank R. Mehta. "The hippocampal rate code: anatomy, physiology and theory." *Trends in neurosciences* 32.6 (2009): 329-338.

Katona, I., et al. "GABAergic interneurons are the targets of cannabinoid actions in the human hippocampus." *Neuroscience* 100.4 (2000): 797-804.

Lee, Sang-Hun, Csaba Földy, and Ivan Soltesz. "Distinct endocannabinoid control of GABA release at perisomatic and dendritic synapses in the hippocampus." *Journal of Neuroscience* 30.23 (2010): 7993-8000.

Lee, Sang-Hun, et al. "Parvalbumin-positive basket cells differentiate among hippocampal pyramidal cells." *Neuron* 82.5 (2014): 1129-1144.

Mátyás, Ferenc, Tamás F. Freund, and Attila I. Gulyás. "Convergence of excitatory and inhibitory inputs onto CCK-containing basket cells in the CA1 area of the rat hippocampus." *European Journal of Neuroscience* 19.5 (2004): 1243-1256.

Ohno-Shosaku, Takako, et al. "Presynaptic cannabinoid sensitivity is a major determinant of depolarization-induced retrograde suppression at hippocampal synapses." *Journal of Neuroscience* 22.10 (2002): 3864-3872.

Pouille, Frédéric, and Massimo Scanziani. "Enforcement of temporal fidelity in pyramidal cells by somatic feed-forward inhibition." *Science* 293.5532 (2001): 1159-1163.

Ruehle, Sabine, et al. "The endocannabinoid system in anxiety, fear memory and habituation." *Journal of Psychopharmacology* 26.1 (2012): 23-39.

Steindel, Frauke, et al. "Neuron-type specific cannabinoid-mediated G protein signalling in mouse hippocampus." *Journal of neurochemistry* 124.6 (2013): 795-807.

1 **Cannabinoids Disrupt Memory Encoding by**
2 **Functionally Isolating Hippocampal CA1 from CA3**

3 Roman A. Sandler *¹, Dustin Fetterhoff ², Robert E. Hampson ², Sam A.
4 Deadwyler ² & Vasilis Z. Marmarelis¹

5 ¹Department of Biomedical Engineering, University of Southern
6 California, Los Angeles, CA, USA

7 ²Department of Physiology & Pharmacology, Wake Forest University,
8 Winston-Salem, NC, USA

9 April 9, 2017

10 **Abstract**

11 *Much of the research on cannabinoids (CBs) has focused on their ef-
12 fects at the molecular and synaptic level. However, the effects of CBs on the
13 dynamics of neural circuits remains poorly understood. This study aims to
14 disentangle the effects of CBs on the functional dynamics of the hippocam-
15 pal Schaffer collateral synapse by using data-driven nonparametric mod-
16 eling. Multi-unit activity was recorded from rats doing a working memory
17 task in control sessions and under the influence of exogenously administered
18 tetrahydrocannabinol (THC), the primary CB found in marijuana. It was
19 found that THC left firing rate unaltered and only slightly reduced theta os-
20 cillations. Multivariate autoregressive models, estimated from spontaneous
21 spiking activity, were then used to describe the dynamical transformation
22 from CA3 to CA1. They revealed that THC served to functionally isolate
23 CA1 from CA3 by reducing feedforward excitation and theta information
24 flow. The functional isolation was compensated by increased feedback exci-
25 tation within CA1. Finally, both of these effects were shown to be correlated
26 with memory impairments in the working memory task. By elucidating the
27 circuit mechanisms of CBs, these results help close the gap in knowledge
28 between the cellular and behavioral effects of CBs.*

29 **Author Summary**

30 Research into cannabinoids (CBs) over the last several decades has found that
31 they induce a large variety of oftentimes opposing effects on various neuronal
32 receptors and processes. Due to this plethora of effects, disentangling how CBs
33 influence neuronal circuits has proven challenging. This paper contributes to our
34 understanding of the circuit level effects of CBs by using data driven modeling to
35 examine how THC affects the input-output relationship in the Schaffer collateral
36 synapse in the hippocampus. It was found that THC functionally isolated CA1
37 from CA3 by reducing feedforward excitation and theta information flow while
38 simultaneously increasing feedback excitation within CA1. By elucidating the
39 circuit mechanisms of CBs, these results help close the gap in knowledge between
40 the cellular and behavioral effects of CBs.

*Corresponding Author: rsandler00@gmail.com

41 1 Introduction

42 Recent years have seen a resurgence of interest in the therapeutic role of cannabinoids (CBs) for several diseases and neurophyschiatric disorders such as psychosis, anxiety disorders, PTSD, and multiple sclerosis [1, 2]. In particular, CB agonists have shown promising but mixed results in the treatment of epilepsy, as various types of agonists at various doses have been shown to be both pro- and anticonvulsant [3, 4, 5, 6, 7, 8, 7]. Parallel to increasing therapeutic research, much work has been done on the chemical structure of various cannabinoids and cannabinoid receptors, along with their cellular interactions and pharmacology [9].

51 Nonetheless, between the large bodies of literature on cannabinoids from chemical, disease, and behavioral perspectives, much less work has been done to explore the effects of cannabinoids on the neural circuit level. This is particularly important since a wide range of complex and often opposing effects have been attributed to cannabinoids on a molecular and cellular level. For example, cannabinoid activation of CB1 receptors, which are found on both pyramidal cells and interneurons, reduces the quantity of neurotransmitter released during an action potential; consequently, increased extracellular cannabinoid levels reduce both excitatory (glutamatergic) and inhibitory (GABAergic) transmission [10]. Furthermore, cannabinoids have been shown to interact with astrocytes [11], mitochondria [12], glycine receptors [13], vanilloid receptors [14], potassium ion channels [15], and to reduce GABA and glutamate reuptake [16, 17]. Consequently, it is very difficult to extrapolate the emergent network level changes simply from a catalogue of effects cannabinoids have a cellular/molecular level.

65 Here, we studied the effects of Δ^9 -tetrahydrocannabinol (THC) on hippocampal networks during memory encoding using spiking activity recorded in rodents in-vivo performing the Delayed-NonMatch-to-Sample (DNMS) working memory task. Multivariate autoregressive (MVAR) models were used in both control and THC sessions to estimate feedforward and feedback dynamical filters, which are akin to the waveform shapes of the CA3 \rightarrow CA1 EPSP and CA1 afterhyperpolarization, respectively [18]. MVAR models, which are a type of linear nonparametric model, are 'data-driven' in the sense that they estimate model parameters directly from recorded neural spiketrains and, unlike more biologically realistic models, make very few *a priori* assumptions on the nature of the neural dynamics [19, 20]. This characteristic makes them particularly well suited for this study, since as previously mentioned the emergent effects of THC on neural circuits are highly complex and unclear. Overall our results suggest that cannabinoids impair memory encoding by functionally isolating CA1 from CA3 via reduced theta information flow and altered excitatory-inhibitory balance across the Schaffer collateral synapse.

81 **2 Results**

82 **2.1 Changes in rate and temporal coding under Cannabinoids**

83 To evaluate the effects of exogenous cannabinoids on the hippocampal network
84 1 mg/kg THC was injected intraperitoneally into $N = 6$ rodents during cer-
85 tain sessions while they were performing a DNMS task (Fig. S1). All data was
86 previously used in a study on the effects of cannabinoids on hippocampal mul-
87 tifractality [21, 22]. Briefly, in the sample phase, the rats were presented one
88 of two levers. After a variable length delay, both levers were presented in the
89 match phase and the rat had to choose the opposite lever to receive a reward.
90 On the behavioral level, it was found that THC impaired rodent-performance
91 on the DNMS task by $12.2 \pm .6\%$ (Fig. 1a, [23]).

92 While performing the DNMS task, single-unit activity was recorded from the
93 hippocampal CA3 and CA1 regions using a multi-electrode array. There were no
94 significant mean firing rate (MFR) differences between THC sessions and control
95 sessions in either CA3 or CA1 cells ($P = .502$, Fig. 1b). No MFR differences were
96 seen whether considering the entire session or only times around the DNMS
97 sample phase, or whether considering all cells or only sample-presentation cells
98 (see below). The lack of any cannabinoid-induced changes in firing rates at this
99 dosage has been observed in previous studies [24, 25].

100 Two types of temporal coding were identified in the recorded spiketrains.
101 First, on slower timescales, several neurons fired preferentially in response to
102 lever presentation in the sample phase of the DNMS task [26]. It was found that
103 THC reduced the proportion of these sample-presentation cells in both CA3 and
104 CA1 by roughly equal amounts ($\Delta = 13 \pm 4\%$, $P < .001$; Fig. 1c). Interestingly,
105 some sample-presentation cells lost all of their preferential firing in THC sessions
106 (Fig. 1d); this contrasts with place cells whose receptive field stays largely intact
107 under cannabinoids [27]. There was an insignificant trend connecting sample-
108 presentation cell reduction with behavioral deficits ($R^2 = .27$, $P = .052$, Fig.
109 S3a).

110 On faster timescales, it was found that several CA3 and CA1 neurons had
111 theta band rhythmicity (4-7 Hz). Hippocampal theta oscillations are known to
112 be intimately related to cognitive function [28, 29, 30] and have previously been
113 linked to performance in the DNMS task [31]; furthermore, theta oscillations are
114 known to be reduced by systemic injections of cannabinoids on both the single
115 unit [24] and network level [32]. It was found that CA1 theta power was slightly
116 but significantly reduced in THC sessions ($\Delta = 2.52\%$, $CI : [.61, 4.4]\% P = .004$;
117 Fig. 1e). A similar theta power reduction was seen in CA3 cells ($\Delta = 1.94\%$,
118 $P = .045$; Fig. S2). Unlike previous results in a different task [24], the reduction
119 in CA1 theta power was not found to be correlated with behavioral deficits in
120 the DNMS task ($P = .674$, Fig. S3b).

121 Overall, these results show that THC has minor effects on the actual neuronal
122 spiketimes: quantity of spikes (MFR) was not affected and spike rhythmicity
123 (theta oscillations) were only slightly affected. Furthermore behavioral deficits
124 induced by cannabinoids could not be explained by any of these factors, which
125 are the traditional markers of rate and temporal coding in the hippocampus.

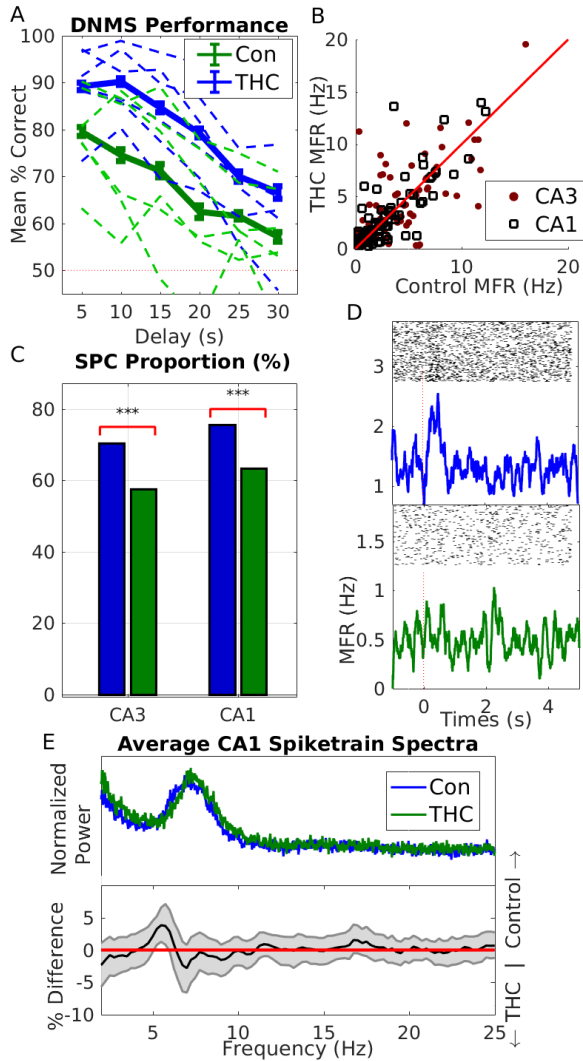


Figure 1: (A) Behavioral performance on Delayed-NonMatch-to-Sample (DNMS) task in both control and THC sessions. Dashed lines show individual animal performance, while solid lines show mean performance over all animals. Bars indicate SEM. Dashed red line indicates performance at chance level. (B) Individual neuron mean firing rate (MFR). (C) Sample-presentation cell (SPC) proportion in CA3 and CA1 cells in control & THC sessions (D) Example of a sample-presentation cell in a control session (top) which lost its firing specificity under THC (bottom). X-axis shows MFR (Hz) (E) Average CA1 spiketrain spectra (top). Bottom shows mean difference in individual cell spectra (thus it is not simply the difference between the signals in above which are averaged over whole population). Gray error bounds indicate 99% confidence bounds. In (B) and (E), only neurons recorded in at least one control & THC session were included. Results for neurons recorded in several control or THC sessions were averaged over those sessions.

126 **2.2 Systems Analysis**

127 The remainder of the study will focus on systems analysis of the Schaffer col-
128 lateral synapse connecting CA3 to CA1, and how this synapse is affected by
129 THC. Systems analysis aims to identify the input-output "blackbox" by which
130 the input spiketrains are transformed into the output spiketrain. On a more
131 abstract level, it aims to identify how the information encoded in CA3 is prop-
132 agated into CA1. This is distinct from the *signal* analysis done in the previous
133 section which only looks at features of individual spiketrains rather than the
134 causal relationship between multiple spiketrains as done in systems analysis.

135 The relationship between an arbitrary number of input CA3 spiketrains
136 and the output CA1 spiketrain was modeled using a multivariate autoregres-
137 sive model described by Eq. 1 and an example of which is pictured in Fig.
138 2a. Each system consists of N input CA3 neurons and N feedforward filters
139 describing the dynamical input-output relationship between the given CA3 and
140 CA1 neurons (Fig. 2b). Intuitively, these filters can be thought of as the EPSP
141 elicited in the output CA1 neuron in response to an action potential (AP) in
142 the input CA3 neuron. However, unlike EPSPs which traditionally only encap-
143 sulate ion-conductances from neurotransmitter-gated ion channels, the "black-
144 box" nature of the feedforward filters means they also include more complex
145 dynamical effects such as dendritic integration, spike generation, active mem-
146 brane conductances, and feedforward interneuronal inhibition (thereby allowing
147 the filters between two pyramidal cells to be inhibitory). Each model also in-
148 cludes a feedback (autoregressive) filter which describes the effects of past output
149 spikes onto the output present. This filter, which can be intuitively thought of
150 as the afterhyperpotential (AHP) [33] includes intracellular processes such as
151 the absolute and relative refractory periods, slow potassium conductances, and
152 I_h conductances. It also includes more complex intercellular processes such as
153 the recurrent connections between CA1 pyramidal cells and interneurons [34].
154 Neuronal connectivity was estimated using a stepwise input selection procedure.
155 Filters were estimated with Laguerre basis expansion using neuronal activity
156 around the sample phase. Model significance was verified using ROC plots and
157 shuffling methods (see supplementary methods).

158 A representative connectivity grid from a recorded THC session with 10
159 recorded neurons (4 CA3, 6 CA1) is shown in Fig. 2a. Fig. 2b shows a sample
160 system from this session between 3 CA3 pyramidal cells and 1 CA1 pyramidal
161 cell. Note that two of the feedforward filters are excitatory (above the x-axis)
162 while the third has both excitatory and inhibitory components, presumably aris-
163 ing through feedforward inhibition involving interneurons [35, 36]. The system
164 also involves a feedback filter which shows a relatively long refractory period
165 ($\sim 40\text{ms}$) followed oscillatory bursting activity. Oscillations in the CA1 pyrami-
166 dal cell AHP are a well known phenomena caused by slow K^+ and I_h conduc-
167 tances, and these oscillations are known to lead to theta resonances [37, 38, 18].
168 In order to study the filter oscillations more closely, the filter frequency spec-
169 tra were plotted in Fig. 2c. Both feedforward excitatory filters were found to
170 have peaks in the high theta range (8-9 Hz). Intuitively, this can be understood

171 to mean that information encoded in the theta range in these input neurons is
 172 preferentially transmitted to the output CA1 neuron. Furthermore, the feedback
 173 filter has a low theta resonance of 3.5 Hz. Significance metrics for the displayed
 174 system are shown in Fig. S4, and additional systems are shown in Fig. S5. All
 175 together 66% (707/1068) of all systems were found to be significant and 2139
 176 feedforward and 707 feedback filters were obtained. THC was found to reduce
 177 the amount of significant models per session ($\Delta = -7.4\%$, $P = .011$), but the
 178 predictive power of significant models, as measured by AUC (see supplementary
 179 methods), was unaltered ($P = .24$).

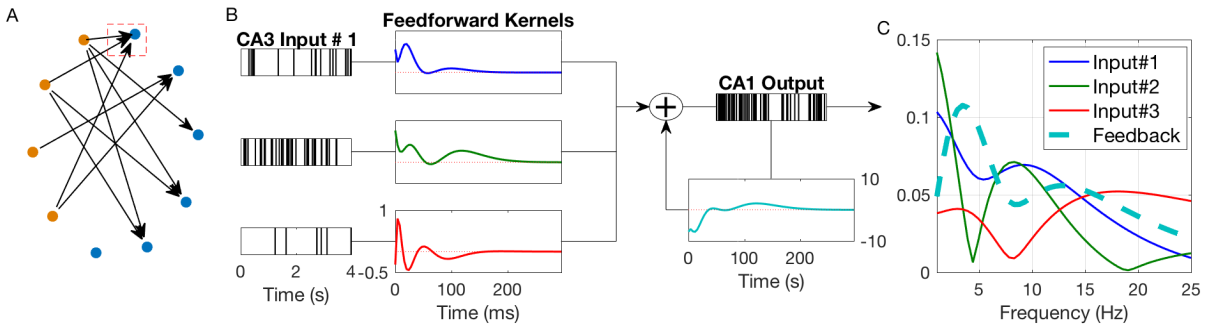


Figure 2: (A) Example connectivity grid of 4 CA3 neurons (orange) and 6 CA1 neurons (blue) recorded during a single session. Note that 1 CA1 neuron has no significant granger-causal inputs. Each line represents a causal connection between those neurons, as encapsulated by a feedforward filter. (B) Example system of CA1 neuron enclosed by the red box in (A). Diagram shows 3 input CA3 spiketrains followed by their respective feedforward filters which are summed with the feedback filter to generate the output CA1 spiketrain. All feedforward filter are plotted with the same y-axis scale. Dashed red line in filter boxes indicates x-axis. (C) Normalized filter spectra computed of feedforward and feedback filters from (B).

180 To study how THC affects system dynamics on a population level, we ex-
 181 amined how features change in the entire sample of control and THC filters.
 182 The average filter frequency profile for both control and THC sessions is shown
 183 in Fig. 3a,b (top). Both feedforward and feedback spectra are found to have
 184 clear theta band peaks, thus generalizing the trend seen in the example system
 185 of Fig. 2. This is consistent previous with reports which show that CA3 prop-
 186 agates strong theta rhythms to CA1 [39, 40] and also that CA1 is capable to
 187 generating endogenous theta rhythms [41]. THC produced a significant decline
 188 in the theta power of the feedback filters ($\Delta = 20.8\%$, $P < .001$; Fig. 3b). Note
 189 that the feedback filter theta reduction is about 10x stronger than the theta
 190 reduction found in the CA1 spiketrain signals (Fig. 1e). No reduction in theta
 191 power was found in the feedforward filters ($P = .61$, Fig. 3a). This result sug-
 192 gests that cannabinoid-induced theta desynchronization results primarily from
 193 altered feedback properties rather than changes in CA3 \rightarrow CA1 dynamics.

194 Cannabinoids have been reported to affect network excitation-inhibition bal-
 195 ance (EIB) [10, 42]. Particularly, there is much debate whether cannabinoids are
 196 pro- or anticonvulsants [8, 43, 44, 4, 6]. In order to examine the effects cannabi-

noids have on network EIB, we quantified the excitation of the estimated filters using a metric called the excitatory index (EI), which is the ratio between positive filter area and total filter area. It was found that THC had no significant effect on feedforward EI ($P = .14$); however, there was an insignificant trend showing that THC-induced decreases in feedforward EI were correlated with behavioral deficits ($R^2 = .27, P = .063$, Fig. 3c). Additionally, THC reduced the amount of causally connected CA3-CA1 neuronal pairs ($\Delta = -8.9\%, P < .001$). These findings, together with the THC-induced decrease of CA3 \rightarrow CA1 significant models, suggest that THC reduces the causal influence CA3 neurons have on CA1 spiketimes. In other words, THC can be said to functionally isolate CA1 from CA3. It was also found that THC significantly increased feedback EI ($\Delta = 3.5\%, P = .022$) and that the increased feedback EI was correlated with behavioral deficits ($R^2 = .38, P = .007$, Fig. 3d).

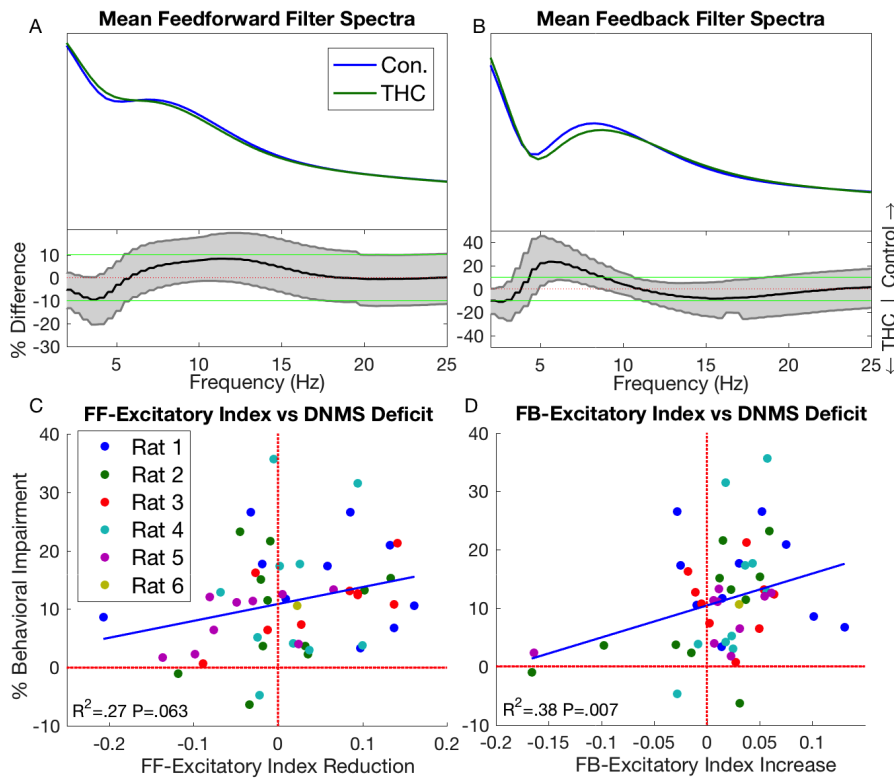


Figure 3: Average feedforward (A) and feedback (B) filter spectra in control and THC sessions (top), and their differences (bottom). Same format and analysis as Fig. 1a. (C) Correlation between feedforward filter excitatory index (EI) reduction and behavioral deficits. Each point represents a specific THC session, with points of the same color coming from the same animal. X-axis shows reduction in feedforward EI, while y-axis shows reduction in behavioral performance. Both reductions were taken relative to control sessions (see supplemental methods). (D) Same as (C) but for feedback EI increase.

210 **2.3 PDM Analysis**

211 The large quantity (>2800) and variability of the obtained filters describing
212 the CA3 \rightarrow CA1 dynamic transformation presents a challenge of interpretation.
213 Namely, how could one identify features from the entire filter population which
214 are representative of the CA3 \rightarrow CA1 transformation rather than just the input-
215 output relationship found in this or that particular pair of neurons. In essence
216 this is an unsupervised learning problem which aims to identify hidden structure
217 within the filter population for the purpose of knowledge discovery. Our group
218 has developed the concept of the global principal dynamic modes (gPDMs) to-
219 wards this effort [19, 45, 46]. The gPDMs are a system-specific and efficient basis
220 set which contain the essential dynamic components of the filter population and
221 are meant to be amenable to biological interpretation. One set of gPDMs were
222 estimated from all (control and THC) obtained filters with the hypothesis that
223 THC would primarily change the expression strength of the gPDMs rather than
224 their specific shapes.

225 Fig. 4a,b shows the obtained feedforward and feedback gPDMs in both the
226 time and frequency domain. Once again, the feedforward and feedback gPDMs
227 represent the dominant independent components of feedforward and feedback
228 kernels, respectively. The first feedforward gPDM was found to have almost all
229 its energy in the 1st time bin, with an immediate decline thereafter. This gPDM
230 represents near concurrent firing between CA3 and CA1 neurons and presum-
231 ably results from both direct CA3 \rightarrow CA1 connections via the Schaffer collateral
232 synapse [47, 48] and common inputs from the entorhinal cortex [49, 50]. The
233 third feedforward gPDM, which is characterized by an initial inhibitory phase,
234 presumably represents feedforward interneuronal inhibition which is prevalent in
235 the CA3 \rightarrow CA1 connection [35, 36]. THC was not found to influence the strength
236 of either of these gPDMs ($P = .76$, $P = .60$; Fig. S6). The second feedforward
237 gPDM which is characterized by sustained and oscillatory excitation was found
238 to have a strong theta peak in the frequency domain. Furthermore, it was found
239 that THC-induced declines in the strength of this gPDM were correlated with
240 behavioral deficits ($R^2 = .30$, $P = .032$; Fig. 4c).

241 The three obtained feedback gPDMs are shown in Fig. 4b. These gPDMs
242 express the essential feedback dynamics found in CA1 neurons. As previously
243 mentioned, these dynamics arise through the combination of intracellular pro-
244 cesses such as the AHP and extracellular processes such as recurrent connections
245 between CA1 pyramidal cells and interneurons. It was found that THC-induced
246 increases in the third feedback gPDM were correlated with behavioral deficits
247 ($R^2 = .39$, $P = .005$; Fig. 4d). This correlation was not seen in either of the first
248 two feedback gPDMs ($P = .32$, $P = .75$; Fig. S6). Notably, the 3rd feedback
249 gPDM was seen to be "theta-blocking" in the frequency domain due to its trough
250 at 8 Hz. This gPDM counteracts the 1st "theta-promoting" feedback gPDM and
251 disrupts theta oscillations in the CA1 neuron. The THC-induced changes in the
252 feedforward and feedback theta gPDMs paint a more complete picture of the
253 CA1 theta reductions seen in Fig. 1e. Namely, they attribute the theta losses
254 to specific feedforward and feedback dynamical filters which may potentially be

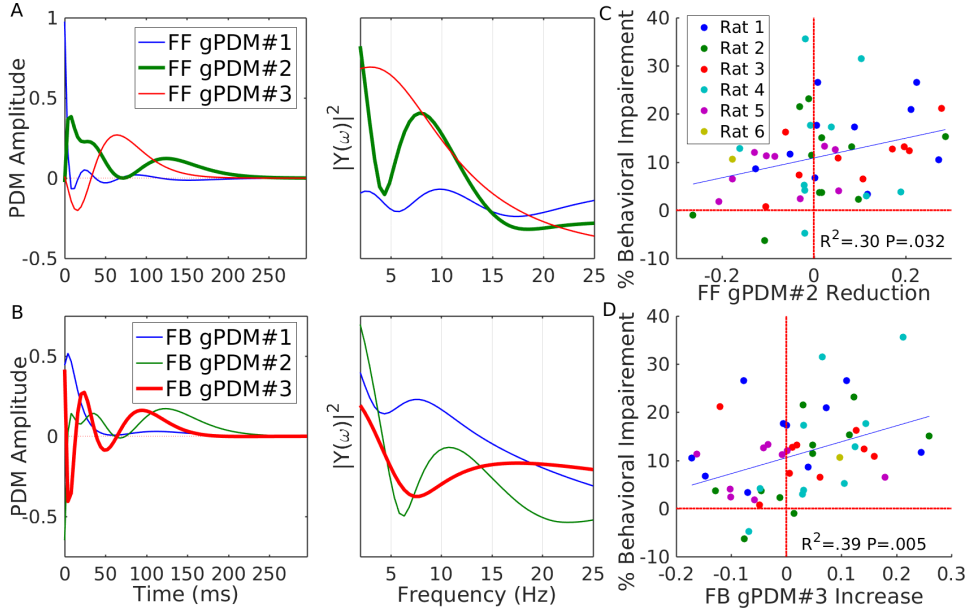


Figure 4: Feedforward (A) and feedback (B) global principal dynamic modes (gPDMs) in both the time (left) and frequency domain (right). Reductions in 2nd feedforward gPDM (C) and increases in 3rd feedback gPDM (D) were found to be correlated with behavioral deficits. Same format as Fig. 3.

traced to specific biophysical mechanisms. Furthermore, changes in these dynamical filters have been specifically correlated with behavioral deficits, which could not be done with theta reductions in the CA1 signal (Fig. S3).

3 Discussion

The current study uses 'data-driven' nonparametric system dynamics modeling tools to study the effects of THC on the Schaffer Collateral synapse in rodents. The chief findings of the study can be summarized as: (1) THC induced little or no change in traditional rate and temporal coding metrics such as MFR and theta power, (2) THC altered the CA1 excitatory-inhibitory balance by reducing feedforward influence from CA3 while increasing feedback excitation in CA1, (3) THC reduced theta information flow through the Schaffer collateral synapse, and (4) the magnitudes of both of the previous effects were directly correlated with the severity of behavioral deficits induced by THC. Overall these results suggest the conclusion that THC impairs memory encoding by functionally isolating CA1 from CA3.

From a computational perspective, the nonparametric modeling methods used in this study proved successful in studying the network level effects of cannabinoids since, unlike biophysical models, all model parameters were estimated directly from recorded data and very few *a priori* assumptions were made about the effects of THC [19, 20, 51]. The global principal dynamic modes (gPDMs), which were derived from MVAR filters of the entire population of neu-

276 rons, further extracted hidden dynamical structure from 'noisy' neuron-neuron
277 variability. Importantly, THC-induced changes in the gPDMs were directly cor-
278 related with behavioral impairments, thus justifying their utility. Furthermore,
279 while most in-vivo studies on THC analyze macro level signals such as LFPs and
280 EEG, this work adds to a relatively small body of literature which analyzes the
281 effects of THC on neuronal population spiking activity. Finally, to our knowl-
282 edge, this is the first work which examines the effect of THC on neuronal systems
283 dynamics, or the causal interactions between signals, rather than on neuronal
284 signals themselves.

285 It was found that THC increased feedback excitatory index in CA1 and that
286 the magnitude of this effect was correlated with behavioral deficits. We hypothe-
287 size that this is due to reduced feedback inhibition from CA1 cholecystokinin
288 (CCK)-containing basket cells. While CCK cells only make up 13.9% of in-
289 terneurons [52], they express significantly more CB1 receptors than any other
290 cell in the hippocampus [53], and their primary output is to CA1 pyramidal cells
291 [52]. Increased THC concentrations would reduce CCK interneuron output by
292 (1) reducing the amount of GABA they release per action potential (2) reducing
293 their MFR due to reduced glutamatergic input from principal cells in both CA3
294 and CA1 [54, 55].

295 It was also found that THC reduced the number of casually connected CA3-
296 CA1 neuronal pairs; furthermore there was an interesting but insignificant trend
297 for THC-induced deficits in feedforward excitation to lead to behavioral deficits.
298 This trend may prove to be significant given a higher sample size. We hypoth-
299 esize that this reduced feedforward influence is caused by decreased glutamate
300 release from CA3 pyramidal cells due to CB1 receptor activation by THC [56].
301 Even though pyramidal cells have much lower densities of CB1 receptors than
302 interneurons [53, 57], there is evidence that CB induced reduction of excita-
303 tion is larger than these relative densities suggest. Principal cells outnumber
304 interneurons 20:1 in CA1 [50] and their CB1 receptors were found to be several
305 fold more efficacious than those of interneurons [58]. Further, lower baseline ac-
306 tivation levels of CB1 receptors on principal cells than on interneurons suggest
307 they would be disproportionately activated by CB agonists [59]. Altogether, the
308 decreased feedback inhibition and feedforward excitation amount to a functional
309 isolation, or breakdown in information flow between CA3 and CA1. We suggest
310 that this functional isolation is responsible for the behavioral impairments seen
311 in the DNMS task.

312 The 'functional isolation' hypothesis is further supported by previous work
313 which showed that the behavioral impairments caused by cannabinoids in the
314 DNMS task were similar to those seen with a full pharmacological lesion of the
315 hippocampus [60] Given the centrality of CA3→CA1 information flow to hip-
316 pocampal function, a functional isolation of these areas could indeed presumably
317 lead to impairments similar to that of a full lesion. Relatedly, Goonawardena
318 et al. [25] injected THC intraperitoneally at low 1 mg/kg doses as in this study
319 and in higher doses of 3 mg/kg. They found that while both doses disrupted
320 hippocampal synchrony, only the higher dose resulted in a reduction in pyrami-
321 dal cell MFR. This suggests that at the lower dose both previously described

322 phenomena are at a net balance, while at the higher dose, the decrease in feed-
323 forward excitation overpowers the increase in feedback excitation and results in
324 lower MFR. Finally, the hypothesis predicts a breakdown in the normal spike-
325 time coordination between pyramidal cells and interneurons in CA1 circuits.
326 The breakdown of this coordination, which has been extensively implicated in
327 hippocampal oscillations [61, 62], could be responsible for the observed decrease
328 in theta oscillations and information flow.

329 Although the current results only suggest this hypothesis, several experi-
330 ments could be done to further substantiate it. Feedforward and feedback ker-
331 nels and gPDMs could be estimated at different doses of THC; the hypothesis
332 would predict that different doses would effect the two processes independently,
333 with one of the two processes potentially being more dominant at different THC
334 levels. Significant developments in *in-vivo* synaptic patch clamping [63] and cal-
335 cium imaging in recent years could be used to directly measure the drive of CCK
336 cells and CA3 pyramidal cells onto CA1 pyramidal cells under THC.

337 Much research has been done investigating the effects THC and other canna-
338 noids have on seizures and epilepsy. Results so far have been mixed, with various
339 studies showing that THC is both pro- and anticonvulsant [3, 4, 5, 6, 7, 8, 7].
340 The results from this study and the presented hypothesis suggest that THC in-
341 herently is not pro- or anti-convulsant but that its effects will depend on the
342 dosage and the unique circuitry of every epileptic focus. Interestingly, a study
343 by Rudenko et al. [6] has shown that indeed the effects of a CB1 agonist were
344 dose dependant, with *lower* doses being anticonvulsant and higher doses being
345 proconvulsant. Finally, this study suggests that in order to truly understand the
346 effects of THC on epileptic circuits, one must study the systems level changes
347 in circuit dynamics rather than taking a reductionist approach and studying the
348 effects of THC on any particular receptor or cell type.

349 The present study analyzed the effects of THC from both a signals and sys-
350 tems perspective - and found that systems analysis yielded much richer results.
351 For example, while analysis of CA1 spiketrain signals showed a slight (2%) re-
352 duction in theta frequency, analysis of system kernels showed that the theta loss
353 was primarily due to CA1 feedback dynamics whose kernels lost over 20% of their
354 theta power, while theta power in feedforward kernels was unaffected. Further-
355 more, only systems analysis allows one to analyze predictive power, feedforward
356 and feedback excitation, and EPSP and AHP waveform shape. Notably, the
357 finding that feedforward influence decreased while feedback excitation increased
358 could not have been observed using only signal analysis which would have only
359 detected a constant MFR.

360 The present study also employed gPDMs as a means to extract the most
361 significant information from the kernel dynamics estimated from several animals
362 over several sessions [19, 64, 18, 48]. The utility of the gPDM method was justi-
363 fied by the finding that reductions in theta related gPDMs in a given session were
364 directly correlated with behavioral deficits, showing that the gPDMs can isolate
365 the particular dynamics which are most affected by THC. Furthermore, THC-
366 induced theta power losses in spiketrain signals were not found to be correlated
367 with behavioral deficits. Although in the present study, kernels and gPDMs were

368 restricted to being linear in order to more easily quantify their overall strength
369 and excitation (via the EI), future work will aim to identify the effects of THC
370 on hippocampal nonlinear dynamics [65, 51].

371 **Ethics Statement**

372 All animal protocols were approved by the Wake Forest University Institutional
373 Animal Care and Use Committee, in accordance with the Association for Assess-
374 ment and Accreditation of Laboratory Animal Care and the National Institute
375 of Health Guide for the Care and Use of Laboratory Animals (NIH Publication
376 No. 8023).

377 **Acknowledgements**

378 This work was supported by NIH (www.nih.gov) grant P41-EB001978 to the
379 Biomedical Simulations Resource at the University of Southern California.

380 **4 Methods**

381 **4.1 Experimental Procedures**

382 N=6 Male Long-Evans rats were trained to criterion on a two lever, spatial
383 Delayed NonMatch-to-Sample (DNMS) task (see Fig. S1). Briefly, during the
384 sample phase the rat was presented one of two levers (left or right). After a delay
385 phase ranging from 1-30 seconds, the rat was presented both levers and had to
386 choose the opposite lever in order to attain a reward. Each rodent underwent 16-
387 25 sessions of the task, which were roughly evenly divided between control and
388 THC sessions, wherein the rodent was intraperitoneally administered 1 mg/kg of
389 body weight Δ^9 -tetrahydrocannabinol (THC), an exogenous cannabinoid found
390 in marijuana. During the task, spike trains were recorded in-vivo with multi-
391 electrode arrays implanted in the left and right CA3 and CA1 regions of the
392 hippocampus. In an effort to acquire a consistent cognitive state, only spiking
393 activity around the sample phase of the task was used. Spikes from multiple
394 trials were sorted, time-stamped, and concatenated into a discretized binary
395 time series using a 4ms bin. For more details on the experimental setup, see
396 supplementary methods.

397 **4.2 Model Configuration and Estimation**

398 Nonparametric multiple-input linear autoregressive models were used to model
399 the dynamical transformation between input and output spike trains (see Fig.
400 2,5) [18, 51]. Each model consisted of a feedforward component, reflecting the
401 effect of the N input cells on the output cell and a feedback (autoregressive)
402 component reflecting the subthreshold and suprathreshold effects the output

403 cell has on itself. Thus, the output $y(t)$ is calculated as:

$$y(t) = \sum_{n=1}^N \sum_{\tau=0}^M k_n(\tau) x_n(t - \tau) + \sum_{\tau=1}^{M+1} k_{AR}(\tau) y(t - \tau) \quad (1)$$

404 where k_n reflects the feedforward filter of input $x_n(t)$, and k_{AR} reflects the feed-
405 back filter. In order to reduce the amount of model parameters and thereby
406 increase parameter stability, we applied the Laguerre expansion technique to ex-
407 pand the feedforward and feedback filters over L Laguerre basis functions (see
408 supplementary methods).

409 Effective connectivity between neurons was assessed using a Granger causality-
410 like approach. For each output CA1 neuron, input CA3 neurons were selected
411 in a forward stepwise procedure whereby only neurons which help predict the
412 output CA1 spike activity were included in the model. After all input neurons
413 were selected, a Monte Carlo approach was used to assess model significance. A
414 model was deemed significant if the CA3 inputs could predict the output CA1
415 activity significantly better ($P < .0001$) than randomly permuted versions of the
416 inputs. See supplementary methods for more details.

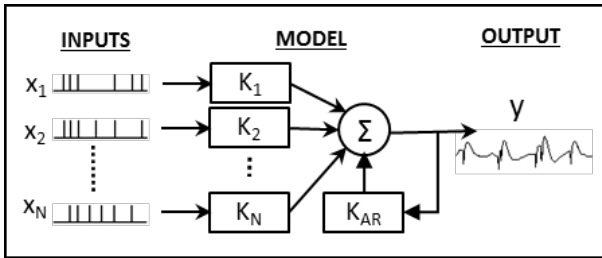


Figure 5: Model Configuration. Each model has N point-process inputs which each go through a linear filter, K_i . These inputs are then summed with the output of the feedback filter, K_{AR} to generate the final output, $y(t)$, which is a continuous signal

417 4.3 Principal Dynamic Modes

418 The global principal dynamic modes (gPDMs) were obtained in a two step pro-
419 cess: first, all filters of each input from every animal were concatenated in a
420 rectangular matrix. Then singular value decomposition (SVD) was performed
421 on the rectangular matrix to obtain all the significant singular vectors, which
422 are the gPDMs. It was found that 3 gPDMs were sufficient to describe the lin-
423 ear dynamics both the population of feedforward and feedback filters. gPDM
424 strength in a given filter was computed by taking the dot product between the
425 gPDM and the filter. gPDM strength in a given session was computed by taking
426 the average gPDM strength in every filter of that session.

427 A Supplementary Methods

428 All data was previously used in a study on the effects of cannabinoids on hip-
429 pocampal multifractality [21, 22])

430 **A.1 Animals**

431 Subjects were Long-Evans rats (Harlan) aged 4–6 months (n = 6) individually
432 housed and allowed free access to food with water regulation to maintain 85% of
433 ad libitum body weight during testing. All animal protocols were approved by
434 the Wake Forest University Institutional Animal Care and Use Committee, in
435 accordance with the Association for Assessment and Accreditation of Laboratory
436 Animal Care and the National Institute of Health Guide for the Care and Use
437 of Laboratory Animals (NIH Publication No. 8023).

438 **A.2 Apparatus**

439 The behavioral testing apparatus for the delayed nonmatch-to-sample (DNMS)
440 task is the same as reported in other studies [23] and consisted of a 43x43x50 cm
441 Plexiglas chamber with two retractable levers (left and right) positioned on either
442 side of a water trough on the front panel. A nosepoke device (photocell) was
443 mounted in the center of the wall opposite the levers with a cue light positioned
444 immediately above the nosepoke device. A video camera was mounted on the
445 ceiling and the entire chamber was housed inside a commercially built sound-
446 attenuated cubicle.

447 **A.3 DNMS Task**

448 The DNMS task consisted of three main phases: Sample, Delay and Nonmatch.
449 The sample phase initiated the trial when either the left or right lever was
450 extended (50% probability), requiring the animal to press it as the Sample Re-
451 sponse (SR). The lever was then retracted and the Delay phase of the task
452 initiated, as signaled by the illumination of a cue light over the nosepoke pho-
453 tocell device on the wall on the opposite side of the chamber. At least one
454 nosepoke (NP) was required following the delay interval which varied randomly
455 in duration (1–30 s) on each trial during the session. The Nonmatch phase began
456 when the delay timed out, the photocell cue light turned off and both the left
457 and right levers on the front panel were extended. Correct responses consisted
458 of pressing the lever in the Nonmatch phase located in the spatial position op-
459 posite the SR (nonmatch response: NR). This produced a drop of water (0.4
460 ml) reward in the trough between the two levers. After the NR the levers were
461 retracted for a 10.0 second intertrial interval (ITI) before the next Sample lever
462 was presented to begin the next trial. A lever press at the same position as the
463 SR (match response) constituted an “error” with no water delivery and turned
464 off of the chamber house lights for 5.0 s and the next trial was presented 5.0 s
465 later. Individual performance was assessed as % NRs (correct responses) with
466 respect to the total number of trials (80–100) per daily (1 hr) sessions.

467 **A.4 Drug Preparation & Administration**

468 Δ^9 -tetrahydrocannabinol (THC) was obtained from the National Institute on
469 Drug Abuse as a 50 mg/ml solution in ethanol. Detergent vehicle was pre-

470 pared from Pluronic F68 (Sigma, St. Louis, MO), 20 mg/ml in ethanol. THC
471 was added to the detergent-ethanol solution (0.5 ml of either THC), and then 2.0
472 ml of saline (0.9%) was slowly added to the ethanol-drug solution. The solution
473 was stirred rapidly and placed under a steady stream of nitrogen gas to evapo-
474 rate the ethanol (~10 min). This resulted in a detergent-drug suspension (12.5
475 mg/ml THC), which was sonicated and then diluted with saline to final injec-
476 tion concentrations (0.5-2.0 mg/ml THC). On drug administration days, animals
477 were injected intraperitoneally with the drug-detergent solution (1 mg/kg) ~10
478 min before the start of the behavioral session. Our experience with these ex-
479 periments has shown that performance after vehicle injection is not significantly
480 different than no injection, and therefore was omitted during this series of ex-
481 periments to minimize risk of infection to the animals. At least two no injection
482 days were imposed between each drug-testing session. All drug solutions were
483 mixed fresh each day.

484 **A.5 Surgery**

485 All surgical procedures conformed to National Institutes of Health and Associa-
486 tion for Assessment and Accreditation of Laboratory Animal Care guidelines,
487 and were performed in a rodent surgical facility approved by the Wake Forest
488 University Institutional Animal Care and Use Committee. After being trained to
489 criterion performance level in the DNMS task animals were anesthetized with ke-
490 tamine (100 mg/kg) and xylazine (10 mg/kg) and placed in a stereotaxic frame.
491 Craniotomies (5mm-diameter) were performed bilaterally over the dorsal hip-
492 pocampus to provide for implantation of 2 identical array electrodes (Neurolinc,
493 New York, NY), each consisting of two rows of 8 stainless steel wires (diameter:
494 20 μm) positioned such that the geometric center of each electrode array was
495 centered at co-ordinates 3.4 mm posterior to Bregma and 3.0 mm lateral (right
496 or left) to midline [66]. The array was designed such that the distance between
497 two adjacent electrodes within a row was 200 μm and between rows was 400
498 μm to conform to the locations of the respective CA3 and CA1 cell layers. The
499 longitudinal axis of the array of electrodes was angled 30° to the midline during
500 implantation to conform to the orientation of the longitudinal axis of the hip-
501 pocampus, with posterior electrode sites more lateral than anterior sites. The
502 electrode array was lowered in 25-100 μm steps to a depth of 3.0 - 4.0 mm from
503 the cortical surface for the longer electrodes positioned in the CA3 cell layer,
504 leaving the shorter CA1 electrodes 1.2 mm higher with tips in the CA1 layer.
505 Extracellular neuronal spike activity was monitored from all electrodes during
506 surgery to maximize placement in the appropriate hippocampal cell layers. After
507 placement of the array the cranium was sealed with bone wax and dental cement
508 and the animals treated with buprenorphine (0.01–0.05 mg/kg) for pain relief
509 over the next 4-6 hrs. The scalp wound was treated periodically with Neosporin
510 antibiotic and systemic injections of penicillin G (300,000 U, intramuscular) were
511 given to prevent infection. Animals were allowed to recover from surgery for at
512 least 1 week before continuing behavioral testing [67].

513 **A.6 Electrophysiological Monitoring & Preprocessing**

514 Animals were connected by cable to the recording apparatus via a 32-channel
515 headstage and harness attached to a 40-channel slip-ring commutator (Crist
516 Instruments, Hagerstown, MD) to allow free movement in the behavioral test-
517 ing chamber. Single neuron action potentials (spikes) were isolated by time-
518 amplitude window discrimination and computer-identified individual waveform
519 characteristics using a multi-neuron acquisition (MAP) processor (Plexon Inc.,
520 Dallas, TX, USA). Single neuron spikes were recorded daily and identified us-
521 ing waveform and firing characteristics within the task (perievent histograms)
522 for each of the DNMS events (SR, LNP & NR). To maintain waveform shape
523 across days, all recorded data was concatenated into one file (separately for each
524 rat) and offline sorting was performed using principal component analysis, peak-
525 valley, and nonlinear energy algorithms in Offline Sorter (Plexon Inc., Dallas,
526 TX, USA). Hippocampal neuron ensembles used to distinguish recording phases
527 and drug treatment conditions consisted of 10-30 single neurons, each recorded
528 from a separate identified electrode location on either of the bilateral arrays.
529 All isolated spike trains contained no less than a 1 ms gap at the center of the
530 autocorrelogram. No effort was made to differentiate between principal cells and
531 interneurons. Previous work has shown that hippocampal neurons recorded with
532 the same waveform from the same electrodes exhibit consistent mean, baseline
533 and DNMS task modulated firing rate alterations [68, 26], and therefore indi-
534 vidual neurons were treated as the same when recorded over multiple days. A
535 total of 189 neurons recorded during 5,143 recording phases were analyzed in
536 the reported experiments.

537 **A.7 Sample-Response Cell Identification**

538 Prior studies from this laboratory have identified hippocampal neurons recorded
539 as above by “Functional Cell Types” (FCTs) described by different behavioral
540 correlates of DNMS task-related events such as lever position and/or phase of
541 the task [26, 25]. Sample-response cells, a subtype of FCTs, were identified by
542 first constructing a smoothed (51 bin) perievent histogram around the sample
543 presentation phase of the DNMS task. The neurons background firing rate mean
544 and variance were calculated from activity 3.5-5s after sample presentation. If
545 the neuron’s MFR from the 2 second window around sample presentation was
546 4 standard deviations greater than its MFR from the background period it was
547 classified as a sample-response cell. It should be noted that for the purpose of
548 this paper other FCTs such as those which respond to a specific lever (left/right)
549 or trial-type cells were not considered [69].

550 **A.8 Laguerre Expansion Technique**

551 In order to apply the Laguerre expansion technique [19], the input and output
 552 data records were first convolved with the Laguerre functions:

$$v_{x_i}^{(l)} = \sum_{\tau=0}^M b_l(\tau) x_i(t - \tau) \quad (2)$$

553

$$v_y^{(l)} = \sum_{\tau=0}^M b_l(\tau) y(t - \tau) \quad (3)$$

554 where b_l is the l^{th} Laguerre basis function. By first convolving with the Laguerre
 555 basis functions, the dynamical effects of the past input epochs are removed and
 556 we are left with a simple regression of contemporaneous data. Substituting the
 557 above equations into equation 1, we have:

$$y(t) = k_0 + \sum_{n=1}^N \sum_{l=1}^L c_{l,x_i}(l) v_{l,x_i}(t) + \sum_{l=1}^L c_{l,y}(l) v_{l,y}(t) \quad (4)$$

558 where c_{l,x_i} and $c_{l,y}$ are the feedforward and feedback Laguerre expansion coeffi-
 559 cients. To estimate model parameters, eq. 4 was cast in matrix form:

$$\mathbf{y} = \mathbf{V}\mathbf{c} + \epsilon \quad (5)$$

560 where \mathbf{y} is the vector of all N output samples, \mathbf{V} is the design matrix consisting
 561 of the convolved inputs, \mathbf{c} are the model parameters to be estimated, and ϵ is
 562 the modeling error. Eq. 5 was solved using least squares regression (LSR). The
 563 memory of our system was fixed at 300ms, in accordance with previous studies
 564 [65, 70]. The Laguerre parameter α was fixed at 0.6 to reflect this system memory
 565 [19].

566 **A.9 Model Selection**

567 In theory, the most predictive model would include all recorded inputs. However,
 568 such a model would be susceptible to overfitting, and would not reveal which
 569 neurons are causally connected to each other. To overcome this issue a forward
 570 step-wise selection procedure was used to minimize overfitting and prune out
 571 all inputs which are not causally related to the output [71]. Given an output
 572 cell and M potential input cells recorded during the same session, the following
 573 steps were used to select the N input cells which are causally connected to the
 574 output cell. First, the data was divided into training (in-sample) and testing
 575 (out-of-sample) sets. Then, M single-input single-output (SISO) models were
 576 constructed with each of the potential inputs. The model whose predicted output
 577 had the highest correlation, as measured by the Pearson correlation-coefficient,
 578 ρ , with the actual output was selected. Afterwards, $N-1$ models were constructed
 579 with two inputs: the previously selected input and one of the remaining potential
 580 inputs. If any of the inputs were able to raise ρ , the input which raised ρ the

581 most was selected; otherwise, the procedure was ended, and only 1 input was
582 selected. This procedure was repeated until either none of the inputs were able
583 to raise ρ , or all M potential neurons were selected. The N selected neurons
584 were then used as the model input.

585 A.10 Model Validation

586 To avoid overfitting, Monte Carlo style simulations were used to select those
587 models which represent significant causal connections between input and output
588 neurons and do not just fit noise [72]. The following procedure was used: in
589 each run the real input was randomly permuted with respect to the output. A
590 model was then generated between the permuted input and the real output, and
591 the Pearson correlation coefficient, ρ_i , was obtained as a metric of performance.
592 T=40 such simulations were conducted for each output and a set of performance
593 metrics, $\{\rho_i\}_i^T$, was obtained. Then, using Fisher's transformation, we tested the
594 hypothesis, H_0 , that ρ was within the population of $\{\rho_i\}$. If this hypothesis could
595 be rejected at the 99.99% significance level, the model was deemed significant.
596 The very conservative threshold ($P < .0001$) was used due to the large amount
597 of comparisons being made.

598 A.11 Statistical Analysis

599 Unless otherwise noted, the unpaired Mann-Whitney U test was used to access
600 whether significant differences exist between two samples. This test was used
601 since it does not assume a normal distribution, and much of our data was found to
602 be skewed/nonnormal. Shift estimates (Hodges-Lehman) and confidence inter-
603 vals were estimated as prescribed by Higgins [73]. In order to estimate the scale
604 estimate, or the ratio between two samples, the data was first log-transformed
605 and then scale estimate was taken to be the antilog of the shift estimate. The
606 χ^2 test was used to compare proportions.

607 In addition to the Pearson correlation coefficient, ρ , Receiver Operating Char-
608 acteristic (ROC) curves were used to visualize model performance. ROC curves
609 plot the true positive rate against the false positive rate over the putative range
610 of threshold values for the continuous output, y [72]. The area under the curve
611 (AUC) of ROC plots are used as a performance metric of the model, and have
612 been shown to be equivalent to the Mann-Whitney two sample statistic [74].
613 The AUC ranges from 0 to 1, with 0.5 indicating a random predictor and higher
614 values indicating better model performance. The ρ and AUC metrics were cho-
615 sen as they measure the similarity between a continuous 'prethreshold' signal
616 and a spike train. The continuous 'prethreshold' signal was chosen over adding
617 a threshold trigger and comparing true output spike train with an output 'post-
618 threshold' spike train for two reasons. First, this allows us to avoid specifying the
619 threshold trigger value, which relies on the somewhat arbitrary tradeoff between
620 true-positive and false-negative spikes [45]. Also, similarity metrics between two
621 spike trains often require the specification of a 'binning parameter' to determine
622 the temporal resolution of the metric [75, 76].

623 **B** Supplementary Figures

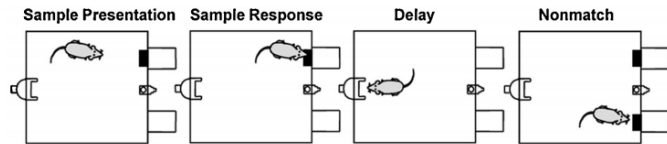


Figure S1: Schematic of the DNMS task. First the rat is presented with one of two levers (sample presentation), which it presses (sample response). Then following a delay phase, the rat is presented with both levers (Nonmatch), of which it must press the opposite lever from which it was presented in order to successfully complete the task.

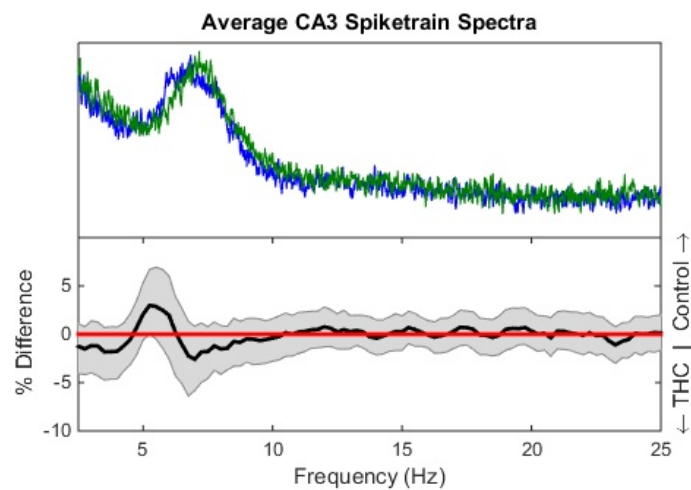


Figure S2: CA3 spectra mean frequency and differences. Same format as Fig. 1e. A weak but significant trend was found for declining CA3 theta oscillations ($\Delta = 1.94\%$, $P = .045$).

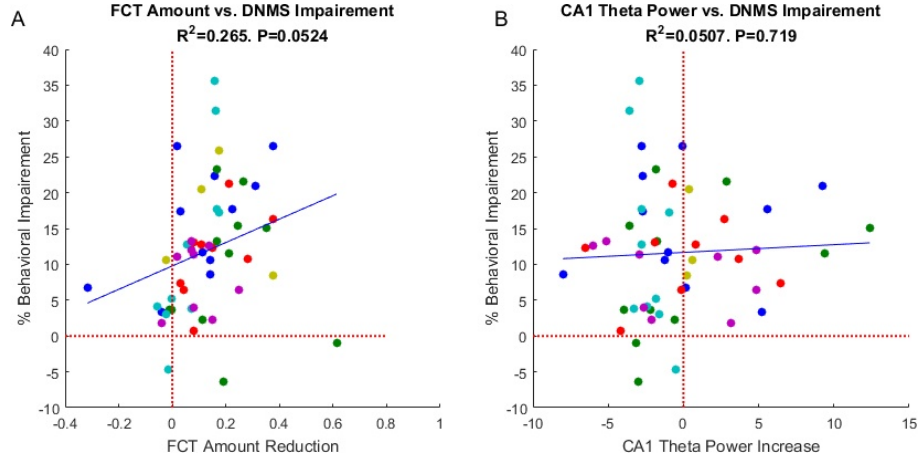


Figure S3: (A) An insignificant trend was found between the THC-induced decrease in the mean number of sample-presentation cells and behavioral performance ($R^2 = .265$, $P = .052$). (B) No relationship was found between reductions in CA1 theta power and behavioral impairment ($P = .67$). Format is same as Fig. 3.

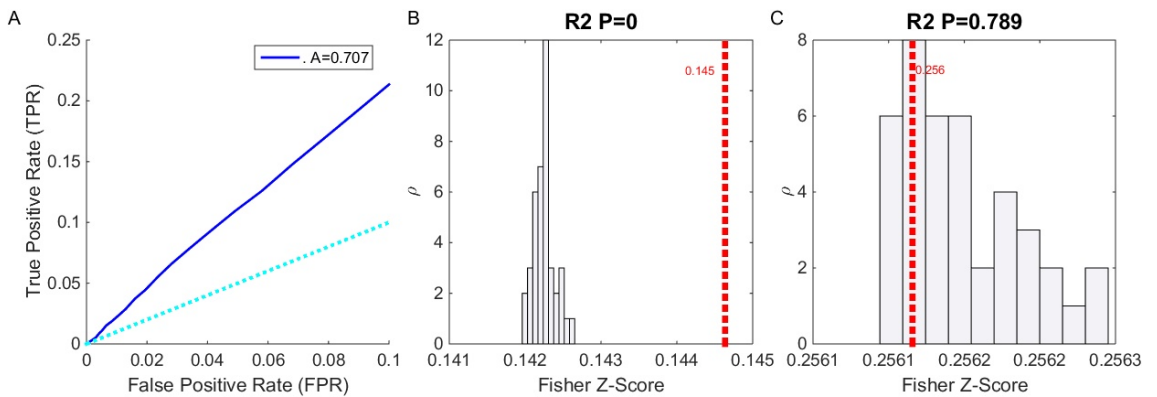


Figure S4: (A) ROC plot (see supplementary methods) for model shown in Fig. 2 showing model predictive power. The light blue line ($TPR=FPR$) indicates a model with no predictive power. (B,C) Examples of Monte Carlo simulations: For each model, 40 surrogate models with shuffled inputs were generated. The Fisher z-scores of these models, which are derived from ρ , were plotted as a histogram, while the true ρ value is the plotted dashed red line. The P value for the hypothesis that the true ρ value is greater than the simulated ρ values is printed above the graphs. Models were deemed significant if $P < .0001$. (B) shows the results for the model in Fig. 2, which was deemed significant. (C) shows an insignificant model

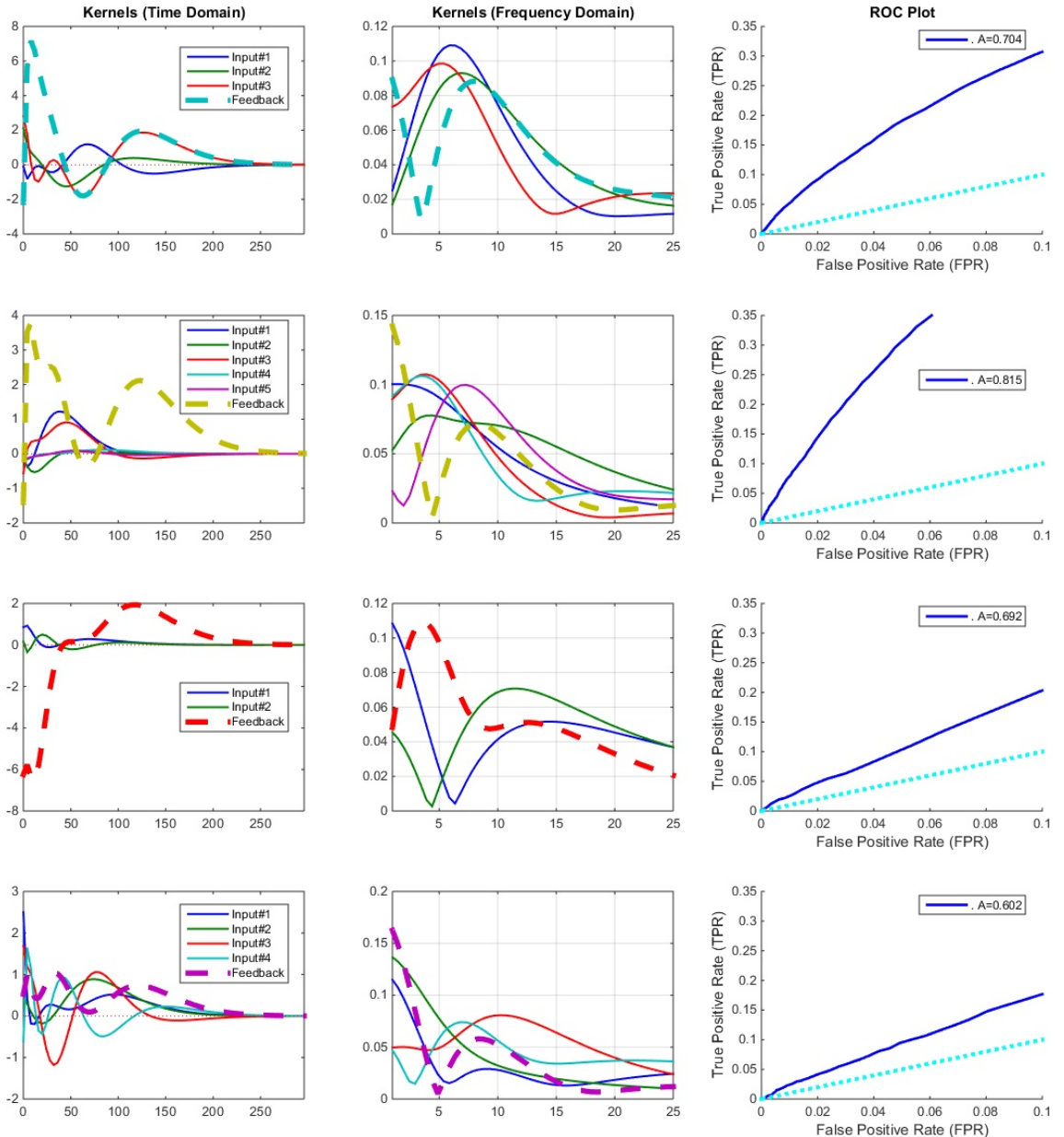


Figure S5: 4 additional systems are presented. Left column shows all system filters, including feedback filter (dashed line) in the time domain. Middle column shows the filters in the frequency domain and right column shows the ROC plots of the models. All these models were found to have significant predictive power in Monte Carlo tests.

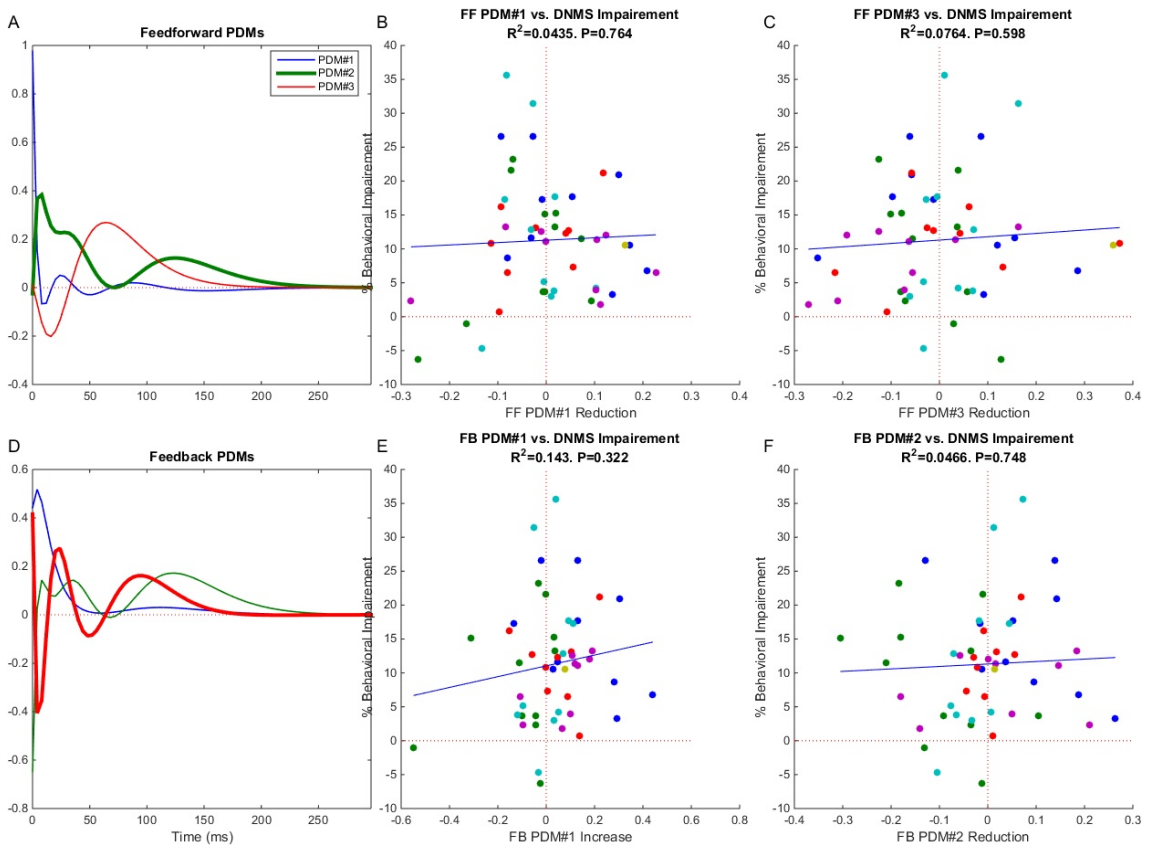


Figure S6: Top Row: neither the first (middle column) nor third feedforward gPDM were found to be significantly correlated with THC induced behavioral deficits. Bottom Row: neither the first (middle column) nor second feedback gPDM were found to be significantly correlated with THC induced behavioral deficits. Format is same as Fig. 3.

624 **References**

- 625 [1] Barbara S Koppel, John CM Brust, Terry Fife, Jeff Bronstein, Sarah Yous-
626 sof, Gary Gronseth, and David Gross. Systematic review: Efficacy and
627 safety of medical marijuana in selected neurologic disorders report of the
628 guideline development subcommittee of the american academy of neurology.
629 *Neurology*, 82(17):1556–1563, 2014.
- 630 [2] Liana Fattore. *Cannabinoids in Neurologic and Mental Disease*. Academic
631 Press, 2015.
- 632 [3] Melisa J Wallace, Jenny L Wiley, Billy R Martin, and Robert J DeLorenzo.
633 Assessment of the role of cb 1 receptors in cannabinoid anticonvulsant ef-
634 ffects. *European Journal of Pharmacology*, 428(1):51–57, 2001.
- 635 [4] Robert E Blair, Laxmikant S Deshpande, Sompong Sombati, Kath-
636 erine W Falenski, Billy R Martin, and Robert J DeLorenzo. Activation
637 of the cannabinoid type-1 receptor mediates the anticonvulsant properties
638 of cannabinoids in the hippocampal neuronal culture models of acquired
639 epilepsy and status epilepticus. *Journal of Pharmacology and Experimental
640 Therapeutics*, 317(3):1072–1078, 2006.
- 641 [5] Laxmikant S Deshpande, Sompong Sombati, Robert E Blair, Dawn S
642 Carter, Billy R Martin, and Robert J DeLorenzo. Cannabinoid cb1 re-
643 ceptor antagonists cause status epilepticus-like activity in the hippocampal
644 neuronal culture model of acquired epilepsy. *Neuroscience letters*, 411(1):
645 11–16, 2007.
- 646 [6] V Rudenko, A Rafiuddin, JR Leheste, and LK Friedman. Inverse relation-
647 ship of cannabimimetic (r+) win 55, 212 on behavior and seizure threshold
648 during the juvenile period. *Pharmacology Biochemistry and Behavior*, 100
649 (3):474–484, 2012.
- 650 [7] István Katona. Cannabis and endocannabinoid signaling in epilepsy. In
651 *Endocannabinoids*, pages 285–316. Springer, 2015.
- 652 [8] Andrew J Hill, TD Hill, and B Whalley. The development of cannabinoid
653 based therapies for epilepsy. *Endocannabinoids: molecular, pharmacological,
654 behavioral and clinical features*. bentham science publishers, Oak Park, IL,
655 pages 164–204, 2013.
- 656 [9] Raphael Mechoulam, Lumír O Hanuš, Roger Pertwee, and Allyn C Howlett.
657 Early phytocannabinoid chemistry to endocannabinoids and beyond. *Nature
658 Reviews Neuroscience*, 2014.
- 659 [10] Emma Puighermanal, Arnau Busquets-Garcia, Rafael Maldonado, and
660 Andrés Ozaita. Cellular and intracellular mechanisms involved in the cog-
661 nitive impairment of cannabinoids. *Philosophical Transactions of the Royal
662 Society B: Biological Sciences*, 367(1607):3254–3263, 2012.

- 663 [11] Mathilde Metna-Laurent and Giovanni Marsicano. Rising stars: Modulation
664 of brain functions by astroglial type-1 cannabinoid receptors. *Glia*, 63(3):
665 353–364, 2015.
- 666 [12] Giovanni Bénard, Federico Massa, Nagore Puente, Joana Lourenço, Luigi
667 Bellocchio, Edgar Soria-Gómez, Isabel Matias, Anna Delamarre, Mathilde
668 Metna-Laurent, Astrid Cannich, et al. Mitochondrial cb1 receptors regulate
669 neuronal energy metabolism. *Nature Neuroscience*, 15(4):558–564, 2012.
- 670 [13] Wei Xiong, KeJun Cheng, Tanxing Cui, Grzegorz Godlewski, Kenner C
671 Rice, Yan Xu, and Li Zhang. Cannabinoid potentiation of glycine receptors
672 contributes to cannabis-induced analgesia. *Nature Chemical Biology*, 7(5):
673 296–303, 2011.
- 674 [14] Jessica A Fawley, Mackenzie E Hofmann, and Michael C Andresen.
675 Cannabinoid 1 and transient receptor potential vanilloid 1 receptors dis-
676 cretely modulate evoked glutamate separately from spontaneous glutamate
677 transmission. *The Journal of Neuroscience*, 34(24):8324–8332, 2014.
- 678 [15] Stephanie C Gantz and Bruce P Bean. Cell-autonomous excitation of
679 midbrain dopamine neurons by endocannabinoid-dependent lipid signaling.
680 *Neuron*, 2017.
- 681 [16] Moyra A Coull, Andrew T Johnston, Roger G Pertwee, and Stephen N
682 Davies. Action of δ -9-tetrahydrocannabinol on gaba a receptor-mediated
683 responses in a grease-gap recording preparation of the rat hippocampal slice.
684 *Neuropharmacology*, 36(10):1387–1392, 1997.
- 685 [17] Timothy M Brown, Jonathan M Brotchie, and Stephen M Fitzjohn.
686 Cannabinoids decrease corticostriatal synaptic transmission via an effect
687 on glutamate uptake. *The Journal of Neuroscience*, 23(35):11073–11077,
688 2003.
- 689 [18] Roman A Sandler, Dong Song, Robert E Hampson, Sam A Deadwyler,
690 Theodore W Berger, and Vasilis Z Marmarelis. Model-based assessment of an
691 in-vivo predictive relationship from ca1 to ca3 in the rodent hippocampus.
692 *Journal of Computational Neuroscience*, pages 1–15, 2014.
- 693 [19] Vasilis Z Marmarelis. *Nonlinear dynamic modeling of physiological systems*.
694 Wiley-Interscience, 2004.
- 695 [20] Dong Song, Vasilis Z Marmarelis, and Theodore W Berger. Parametric and
696 non-parametric modeling of short-term synaptic plasticity. part i: Compu-
697 tational study. *Journal of Computational Neuroscience*, 26(1):1–19, 2009.
- 698 [21] Dustin Fetterhoff, Ioan Opris, Sean L Simpson, Sam A Deadwyler, Robert E
699 Hampson, and Robert A Kraft. Multifractal analysis of information pro-
700 cessing in hippocampal neural ensembles during working memory under δ
701 9-tetrahydrocannabinol administration. *Journal of Neuroscience Methods*,
702 2014.

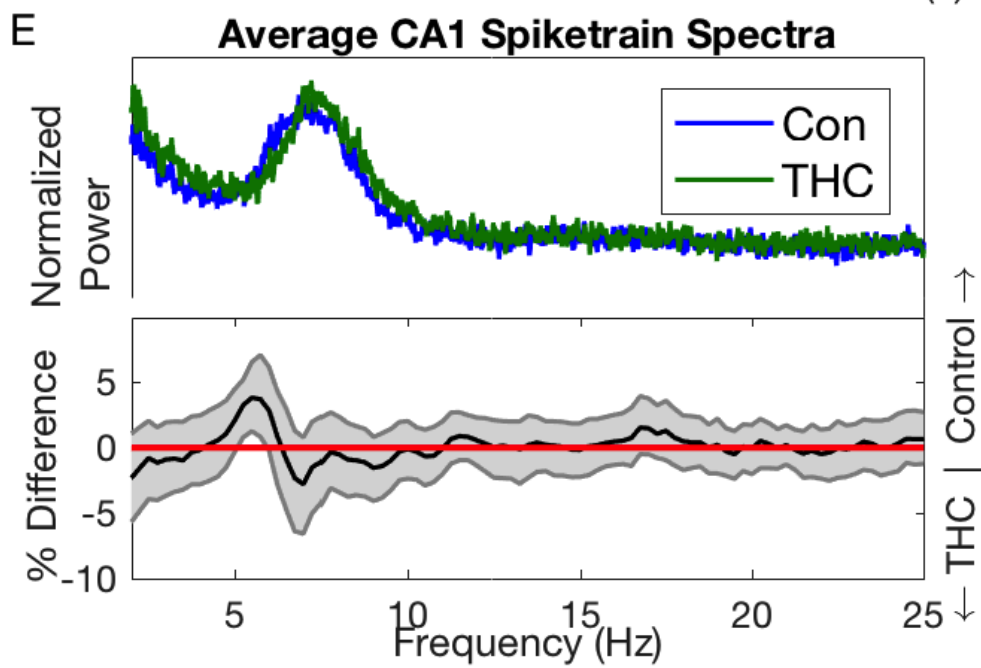
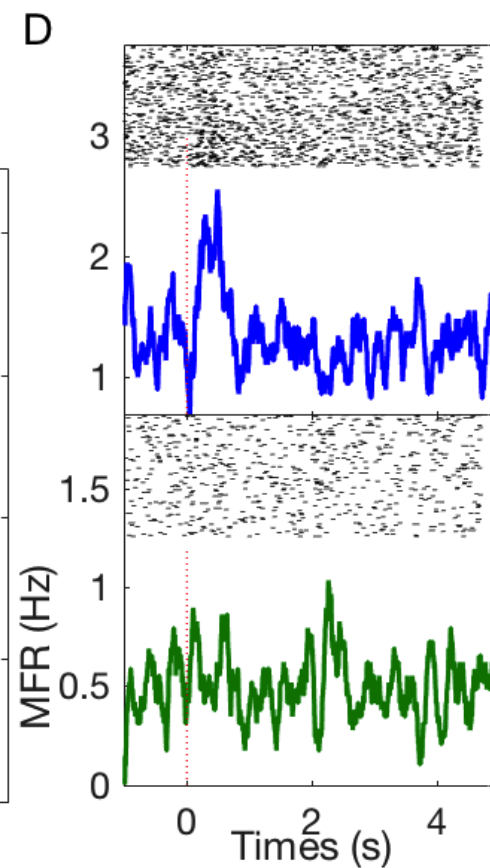
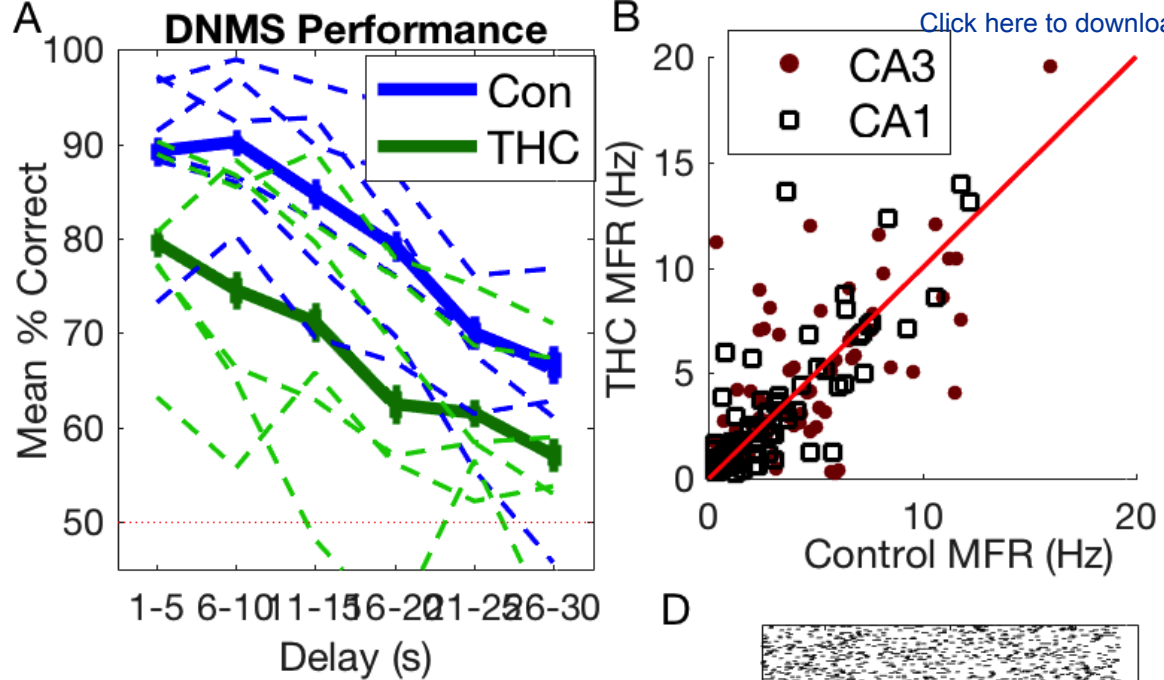
- 703 [22] Dustin Fetterhoff, Robert A Kraft, Roman A Sandler, Ioan Opris, Cheryl A
704 Sexton, Vasilis Z Marmarelis, Robert E Hampson, and Sam A Deadwyler.
705 Distinguishing cognitive state with multifractal complexity of hippocampal
706 interspike interval sequences. *Frontiers in Systems Neuroscience*, 9, 2015.
- 707 [23] Robert E Hampson and Sam A Deadwyler. Cannabinoids reveal the neces-
708 sity of hippocampal neural encoding for short-term memory in rats. *The
709 Journal of Neuroscience*, 20(23):8932–8942, 2000.
- 710 [24] David Robbe, Sean M Montgomery, Alexander Thome, Pavel E Rueda-
711 Orozco, Bruce L McNaughton, and György Buzsaki. Cannabinoids reveal
712 importance of spike timing coordination in hippocampal function. *Nature
713 Neuroscience*, 9(12):1526–1533, 2006.
- 714 [25] Anushka V Goonawardena, Lianne Robinson, Robert E Hampson, and Ger-
715 not Riedel. Cannabinoid and cholinergic systems interact during perfor-
716 mance of a short-term memory task in the rat. *Learning & Memory*, 17
717 (10):502–511, 2010.
- 718 [26] Robert E Hampson, John D Simeral, and Sam A Deadwyler. Distribution
719 of spatial and nonspatial information in dorsal hippocampus. *Nature*, 402
720 (6762):610–614, 1999.
- 721 [27] David Robbe and György Buzsáki. Alteration of theta timescale dynamics
722 of hippocampal place cells by a cannabinoid is associated with memory
723 impairment. *The Journal of Neuroscience*, 29(40):12597–12605, 2009.
- 724 [28] Gyorgy Buzsaki. *Rhythms of the Brain*. Oxford University Press, 2006.
- 725 [29] Laura Lee Colgin. Mechanisms and functions of theta rhythms. *Annual
726 Review of Neuroscience*, 36:295–312, 2013.
- 727 [30] György Buzsáki and Edvard I Moser. Memory, navigation and theta rhythm
728 in the hippocampal-entorhinal system. *Nature Neuroscience*, 16(2):130–138,
729 2013.
- 730 [31] James M Hyman, Eric A Zilli, Amanda M Paley, and Michael E Hasselmo.
731 Working memory performance correlates with prefrontal-hippocampal theta
732 interactions but not with prefrontal neuron firing rates. *Frontiers in Inte-
733 grative Neuroscience*, 4, 2010.
- 734 [32] Mihály Hajós, William E Hoffmann, and Bernát Kocsis. Activation of
735 cannabinoid-1 receptors disrupts sensory gating and neuronal oscillation:
736 relevance to schizophrenia. *Biological psychiatry*, 63(11):1075–1083, 2008.
- 737 [33] N Spruston and C McBain. Structural and functional properties of hip-
738 pocampal neurons. *The Hippocampus Book*, pages 133–201, 2007.
- 739 [34] Thomas Klausberger and Peter Somogyi. Neuronal diversity and temporal
740 dynamics: the unity of hippocampal circuit operations. *Science*, 321(5885):
741 53–57, 2008.

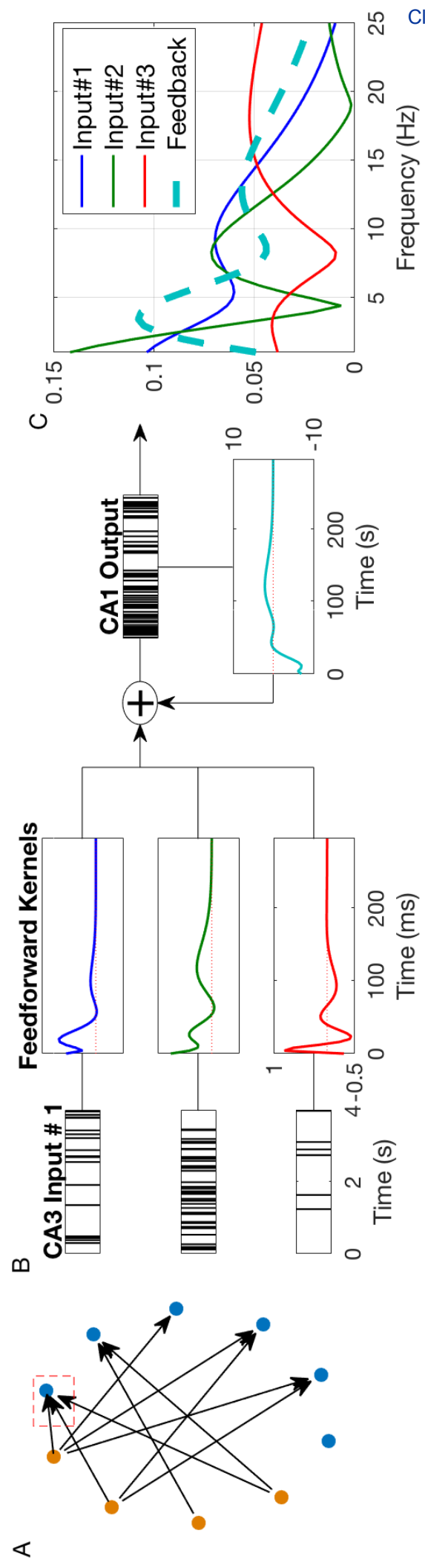
- 742 [35] Frédéric Pouille and Massimo Scanziani. Enforcement of temporal fidelity
743 in pyramidal cells by somatic feed-forward inhibition. *Science*, 293(5532):
744 1159–1163, 2001.
- 745 [36] Rita Zemankovics, Judit M Veres, Iris Oren, and Norbert Hájos. Feedfor-
746 ward inhibition underlies the propagation of cholinergically induced gamma
747 oscillations from hippocampal ca3 to ca1. *The Journal of Neuroscience*, 33
748 (30):12337–12351, 2013.
- 749 [37] L Stan Leung and Hui-Wen Yu. Theta-frequency resonance in hippocampal
750 ca1 neurons in vitro demonstrated by sinusoidal current injection. *Journal*
751 *of neurophysiology*, 79(3):1592–1596, 1998.
- 752 [38] Bruce Hutcheon and Yosef Yarom. Resonance, oscillation and the intrinsic
753 frequency preferences of neurons. *Trends in Neurosciences*, 23(5):216–222,
754 2000.
- 755 [39] Bernat Kocsis, Anatol Bragin, and György Buzsáki. Interdependence of
756 multiple theta generators in the hippocampus: a partial coherence analysis.
757 *The Journal of neuroscience*, 19(14):6200–6212, 1999.
- 758 [40] György Buzsáki. Theta oscillations in the hippocampus. *Neuron*, 33(3):
759 325–340, 2002.
- 760 [41] Romain Goutagny, Jesse Jackson, and Sylvain Williams. Self-generated
761 theta oscillations in the hippocampus. *Nature Neuroscience*, 12(12), 2009.
- 762 [42] Krisztina Monory, Martin Polack, Anita Remus, Beat Lutz, and Martin
763 Korte. Cannabinoid cb1 receptor calibrates excitatory synaptic balance in
764 the mouse hippocampus. *The Journal of Neuroscience*, 35(9):3842–3850,
765 2015.
- 766 [43] SA Turkanis and R Karler. Central excitatory properties of δ 9-
767 tetrahydrocannabinol and its metabolites in iron-induced epileptic rats.
768 *Neuropharmacology*, 21(1):7–13, 1982.
- 769 [44] Angela B Clement, E Gregory Hawkins, Aron H Lichtman, and Benjamin F
770 Cravatt. Increased seizure susceptibility and proconvulsant activity of anan-
771 damide in mice lacking fatty acid amide hydrolase. *The Journal of Neuro-
772 science*, 23(9):3916–3923, 2003.
- 773 [45] Vasilis Z Marmarelis, Dae C Shin, Dong Song, Robert E Hampson, Sam A
774 Deadwyler, and Theodore W Berger. Nonlinear modeling of dynamic inter-
775 actions within neuronal ensembles using principal dynamic modes. *Journal*
776 *of computational neuroscience*, 34(1):73–87, 2013.
- 777 [46] Roman A Sandler and Vasilis Z. Marmarelis. Understanding spike triggered
778 covariance using wiener theory for receptive field identification. *Journal of*
779 *Vision*, in press.

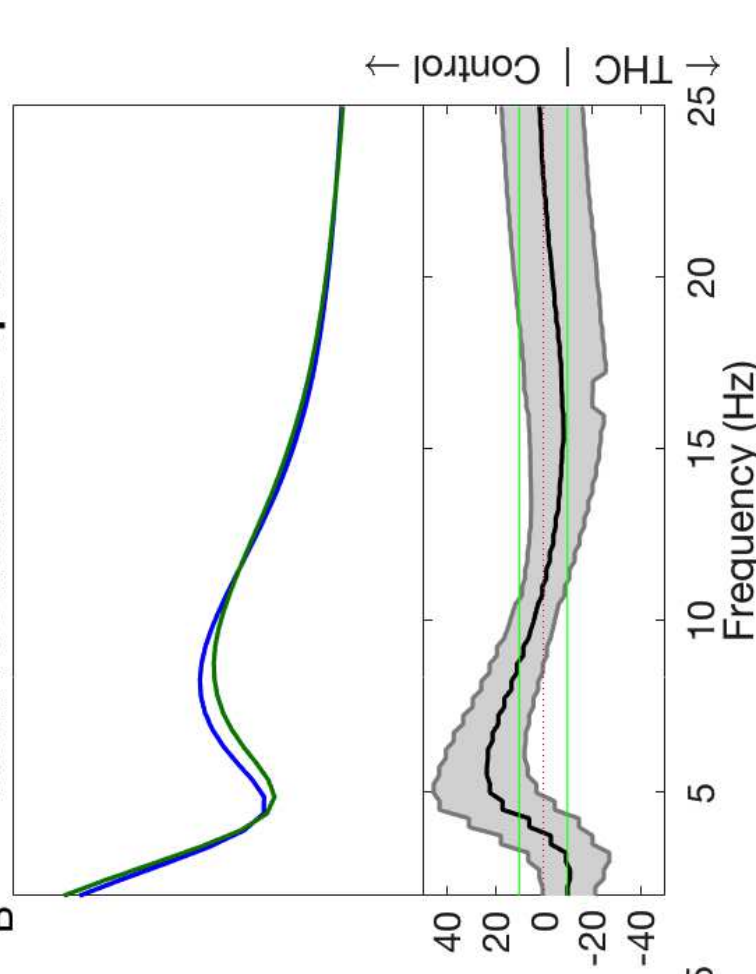
- 780 [47] Sam A Deadwyler, James R West, Carl W Cotman, and Gary Lynch. Physiological studies of the reciprocal connections between the hippocampus and
781 entorhinal cortex. *Experimental Neurology*, 49(1):35–57, 1975.
- 783 [48] Roman A Sandler, Dong Song, Robert E Hampson, Sam A Deadwyler,
784 Theodore W Berger, and Vasilis Z Marmarelis. Closed-loop hippocampal
785 modeling and the design of neurostimulation patterns for suppressing
786 seizures. *Journal of Neural Engineering*, Under Review.
- 787 [49] Roland SG Jones. Entorhinal-hippocampal connections: a speculative view
788 of their function. *Trends in Neurosciences*, 16(2):58–64, 1993.
- 789 [50] Omar J Ahmed and Mayank R Mehta. The hippocampal rate code:
790 anatomy, physiology and theory. *Trends in neurosciences*, 32(6):329–338,
791 2009.
- 792 [51] Roman A Sandler, Samuel A Deadwyler, Robert E Hampson, Dong Song,
793 Theodore W Berger, and Vasilis Z Marmarelis. System identification of
794 point-process neural systems using probability based volterra kernels. *Journal
795 of Neuroscience Methods*, 240:179–192, 2015.
- 796 [52] Marianne J Bezaire and Ivan Soltesz. Quantitative assessment of ca1 local
797 circuits: Knowledge base for interneuron-pyramidal cell connectivity.
798 *Hippocampus*, 23(9):751–785, 2013.
- 799 [53] I Katona, B Sperlagh, Zs Maglóczky, E Santha, A Köfalvi, S Czirjak,
800 K Mackie, ES Vizi, and TF Freund. Gabaergic interneurons are the targets
801 of cannabinoid actions in the human hippocampus. *Neuroscience*, 100(4):
802 797–804, 2000.
- 803 [54] Ferenc Mátyás, Tamás F Freund, and Attila I Gulyás. Convergence of
804 excitatory and inhibitory inputs onto cck-containing basket cells in the ca1
805 area of the rat hippocampus. *European Journal of Neuroscience*, 19(5):
806 1243–1256, 2004.
- 807 [55] Sang-Hun Lee, Csaba Földy, and Ivan Soltesz. Distinct endocannabinoid
808 control of gaba release at perisomatic and dendritic synapses in the hip-
809 pocampus. *Journal of Neuroscience*, 30(23):7993–8000, 2010.
- 810 [56] Maoxing Shen, Timothy M Piser, Virginia S Seybold, and Stanley A Thayer.
811 Cannabinoid receptor agonists inhibit glutamatergic synaptic transmission
812 in rat hippocampal cultures. *The Journal of Neuroscience*, 16(14):4322–
813 4334, 1996.
- 814 [57] Takako Ohno-Shosaku, Hiroshi Tsubokawa, Ichiro Mizushima, Norihide
815 Yoneda, Andreas Zimmer, and Masanobu Kano. Presynaptic cannabinoid
816 sensitivity is a major determinant of depolarization-induced retrograde sup-
817 pression at hippocampal synapses. *Journal of Neuroscience*, 22(10):3864–
818 3872, 2002.

- 819 [58] Frauke Steindel, Raissa Lerner, Martin Häring, Sabine Ruehle, Gio-
820 vanni Marsicano, Beat Lutz, and Krisztina Monory. Neuron-type specific
821 cannabinoid-mediated g protein signalling in mouse hippocampus. *Journal*
822 of *neurochemistry*, 124(6):795–807, 2013.
- 823 [59] Sabine Ruehle, A Aparisi Rey, Floortje Remmers, and Beat Lutz. The
824 endocannabinoid system in anxiety, fear memory and habituation. *Journal*
825 of *Psychopharmacology*, 26(1):23–39, 2012.
- 826 [60] Robert E Hampson and Sam A Deadwyler. Role of cannabinoid receptors
827 in memory storage. *Neurobiology of disease*, 5(6):474–482, 1998.
- 828 [61] Miles A Whittington and Roger D Traub. Interneuron diversity series:
829 Inhibitory interneurons and network oscillations in vitro. *Trends in neuro-*
830 *sciences*, 26(12):676–682, 2003.
- 831 [62] Horacio G Rotstein, Dmitri D Pervouchine, Corey D Acker, Martin J Gillies,
832 John A White, Eberhardt H Buhl, Miles A Whittington, and Nancy Kopell.
833 Slow and fast inhibition and an h-current interact to create a theta rhythm
834 in a model of ca1 interneuron network. *J Neurophysiol*, 94:1509–1518, 2005.
- 835 [63] Can Tao, Guangwei Zhang, Ying Xiong, and Yi Zhou. Functional dissection
836 of synaptic circuits: in vivo patch-clamp recording in neuroscience. *Frontiers*
837 in *Neural Circuits*, 9:23, 2015.
- 838 [64] Vasilis Z Marmarelis, Dae C Shin, Dong Song, Robert E Hampson, Sam A
839 Deadwyler, and Theodore W Berger. On parsing the neural code in the
840 prefrontal cortex of primates using principal dynamic modes. *Journal of*
841 *Computational Neuroscience*, 36(3):321–337, 2014.
- 842 [65] Dong Song, Rosa HM Chan, Vasilis Z Marmarelis, Robert E Hampson,
843 Sam A Deadwyler, and Theodore W Berger. Nonlinear dynamic modeling of
844 spike train transformations for hippocampal-cortical prostheses. *Biomedical*
845 *Engineering, IEEE Transactions on*, 54(6):1053–1066, 2007.
- 846 [66] George Paxinos and CH Watson. The rat brain in stereotaxic coordinates
847 2nd edn. *Academic Press, New York.*, 11(4):237–243, 1986.
- 848 [67] Theodore W Berger, Dong Song, Rosa HM Chan, Vasilis Z Marmarelis, Jeff
849 LaCoss, Jack Wills, Robert E Hampson, Sam A Deadwyler, and John J
850 Granacki. A hippocampal cognitive prosthesis: multi-input, multi-output
851 nonlinear modeling and vlsi implementation. *Neural Systems and Rehabili-*
852 *tation Engineering, IEEE Transactions on*, 20(2):198–211, 2012.
- 853 [68] Sam A Deadwyler, Terence Bunn, and Robert E Hampson. Hippocampal
854 ensemble activity during spatial delayed-nonmatch-to-sample performance
855 in rats. *Journal of Neuroscience*, 16(1):354–372, 1996.
- 856 [69] Robert E Hampson, Dong Song, Rosa HM Chan, Andrew J Sweatt,
857 Mitchell R Riley, Anushka V Goonawardena, Vasilis Z Marmarelis, Greg A

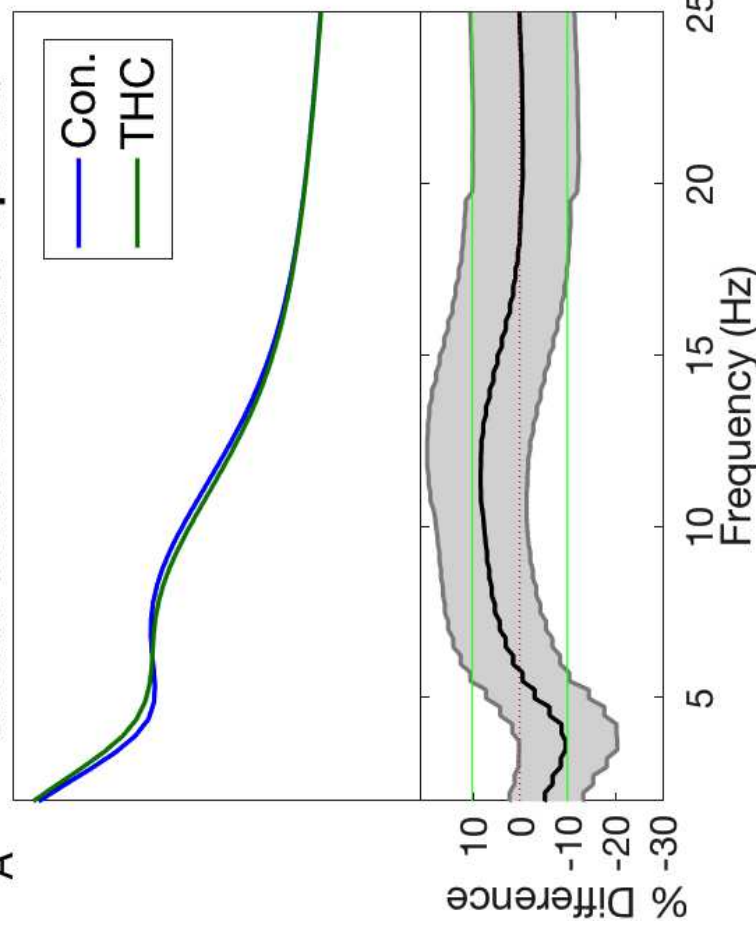
- 858 Gerhardt, Theodore W Berger, and Sam A Deadwyler. Closing the loop
859 for memory prosthesis: Detecting the role of hippocampal neural ensembles
860 using nonlinear models. *Neural Systems and Rehabilitation Engineering,*
861 *IEEE Transactions on*, 20(4):510–525, 2012.
- 862 [70] Ude Lu, Dong Song, and Theodore W Berger. Nonlinear dynamic modeling
863 of synaptically driven single hippocampal neuron intracellular activity.
864 *Biomedical Engineering, IEEE Transactions on*, 58(5):1303–1313, 2011.
- 865 [71] Dong Song, Rosa HM Chan, Vasilis Z Marmarelis, Robert E Hampson,
866 Sam A Deadwyler, and Theodore W Berger. Nonlinear modeling of neural
867 population dynamics for hippocampal prostheses. *Neural Networks*, 22(9):
868 1340–1351, 2009.
- 869 [72] Theodoros P Zanos, Spiros H Courellis, Theodore W Berger, Robert E
870 Hampson, Sam A Deadwyler, and Vasilis Z Marmarelis. Nonlinear modeling
871 of causal interrelationships in neuronal ensembles. *Neural Systems and*
872 *Rehabilitation Engineering, IEEE Transactions on*, 16(4):336–352, 2008.
- 873 [73] James J. Higgins. *Intoruction to Modern Nonparametric Statistics*. 2003.
- 874 [74] James A Hanley and Barbara J McNeil. The meaning and use of the area
875 under a receiver operating characteristic (roc) curve. *Radiology*, 143(1):
876 29–36, 1982.
- 877 [75] Mark CW van Rossum. A novel spike distance. *Neural Computation*, 13
878 (4):751–763, 2001.
- 879 [76] Jonathan D Victor and Keith P Purpura. Metric-space analysis of spike
880 trains: theory, algorithms and application. *Network: computation in neural*
881 *systems*, 8(2):127–164, 1997.



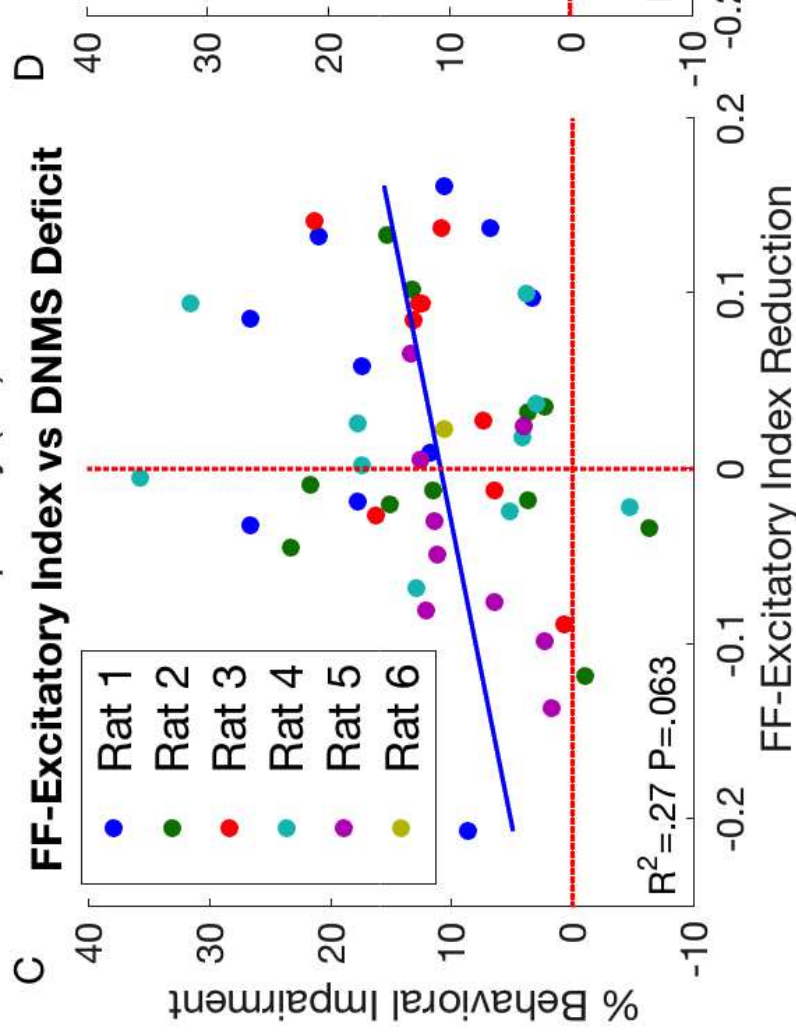
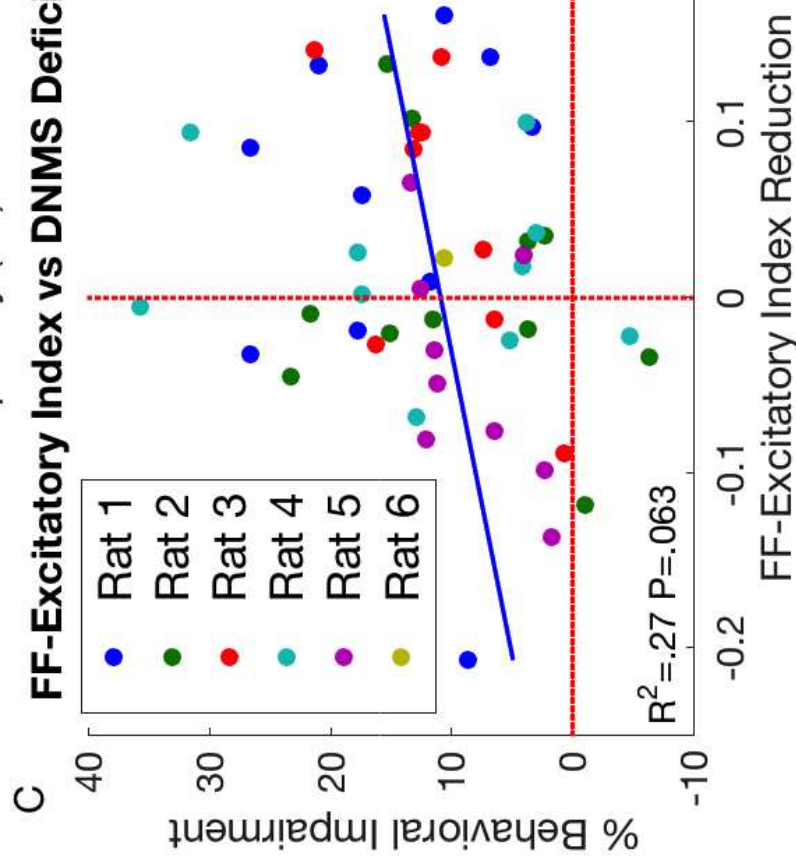


Mean Feedback Filter Spectra

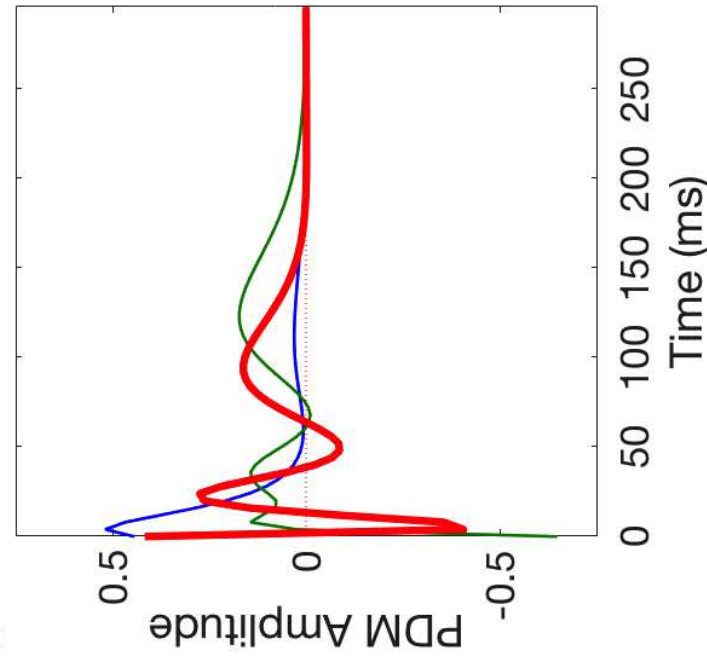
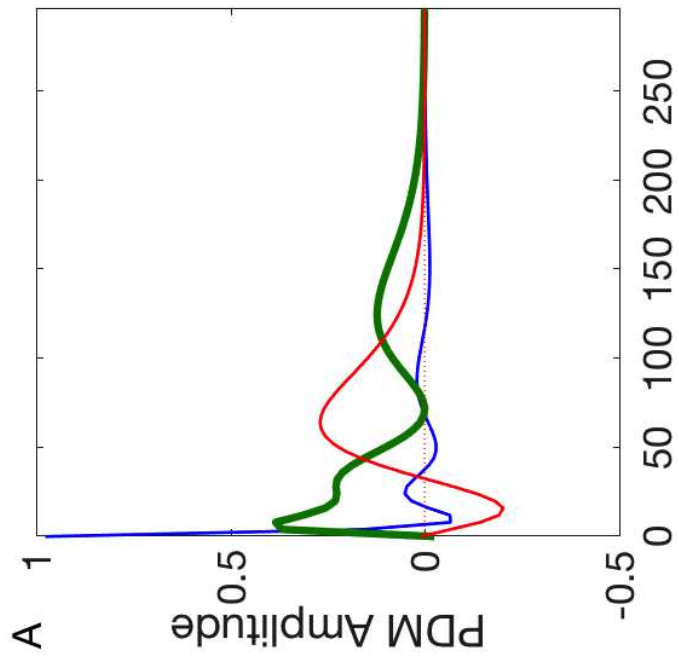
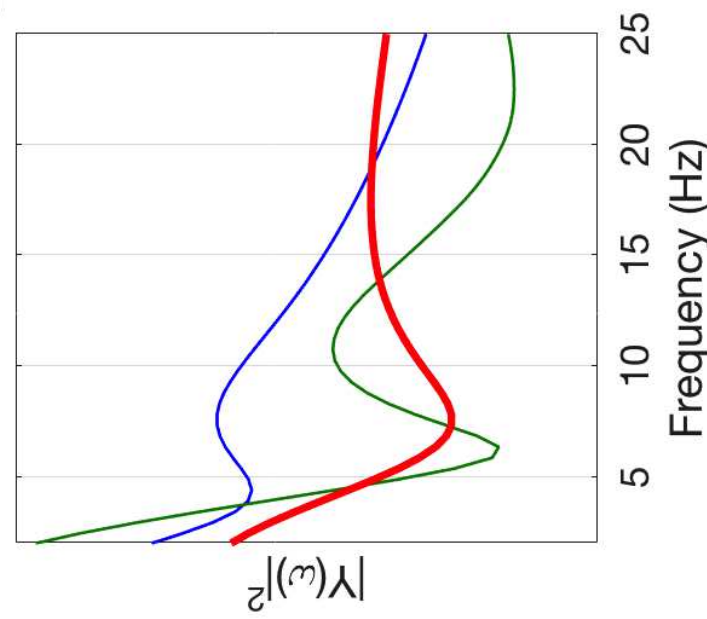
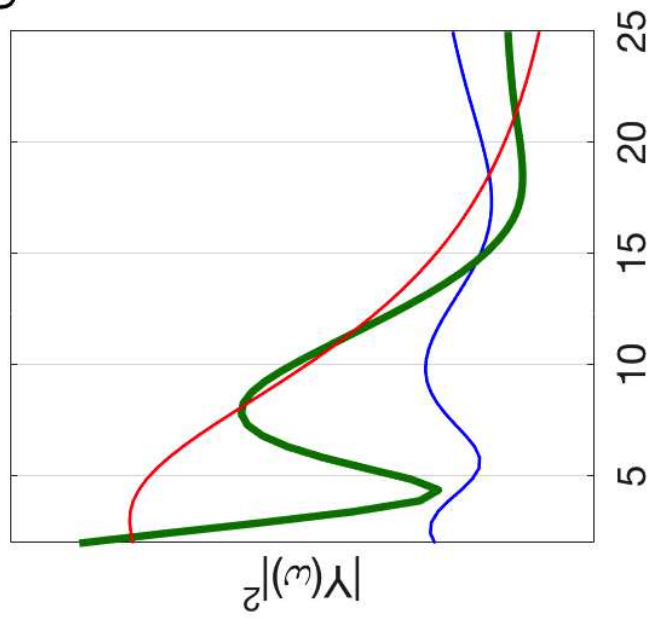
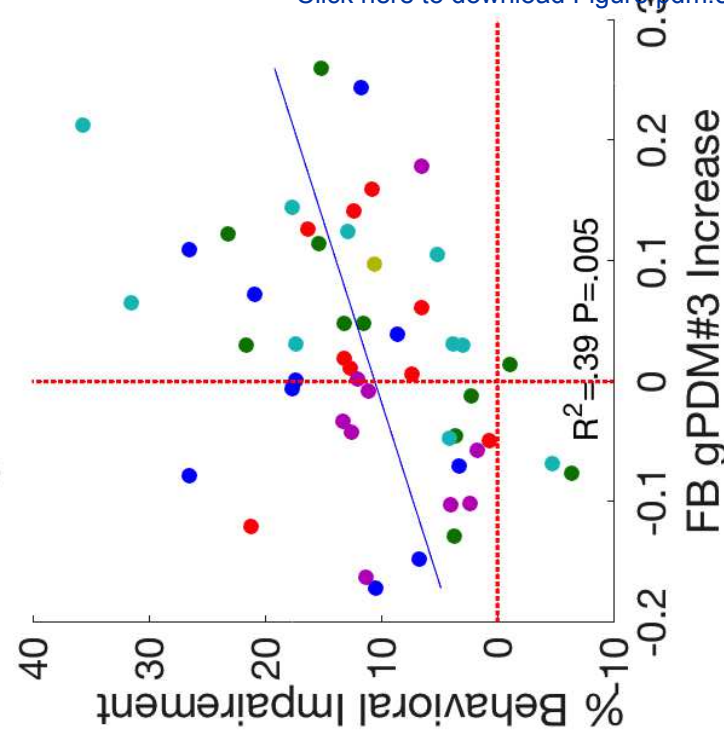
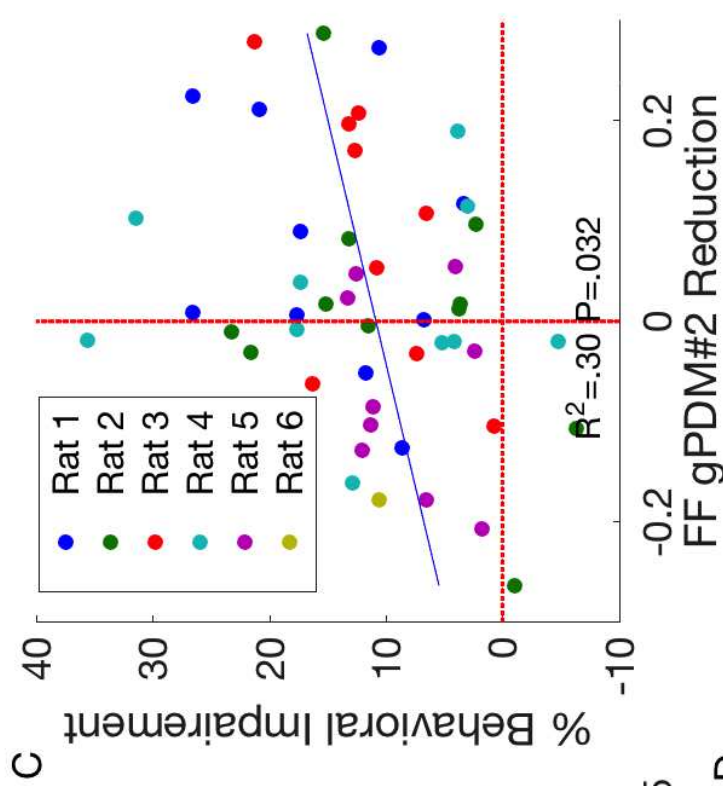
B

Mean Feedforward Filter Spectra

A

FB-Excitatory Index vs DNMS Deficit**FF-Excitatory Index vs DNMS Deficit**

- Rat 1
- Rat 2
- Rat 3
- Rat 4
- Rat 5
- Rat 6





Click here to access/download
Supporting Information
Supp-Methods.tex



Click here to access/download
Supporting Information
DNMS.eps



Click here to access/download
Supporting Information
SFca3spectra.eps



Click here to access/download
Supporting Information
SFnegsig.eps



Click here to access/download
Supporting Information
SFMCsig.eps



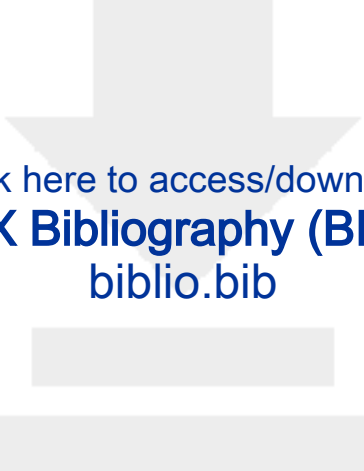
Click here to access/download
Supporting Information
SF_MVARxtra.eps



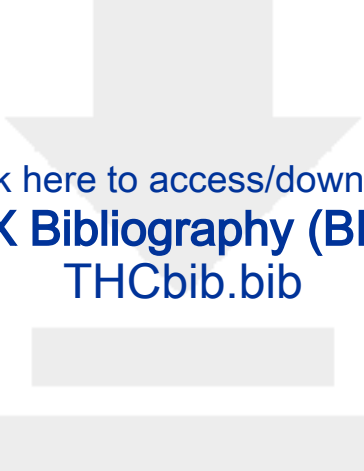
Click here to access/download
Supporting Information
SFnegpdm.eps



Click here to access/download
LaTeX Source File (TEX file)
THC.tex



Click here to access/download
LaTeX Bibliography (BIB file)
biblio.bib



Click here to access/download
LaTeX Bibliography (BIB file)
THCbib.bib